Kütahya Dumlupınar University
Institute of Graduate Studies

Journal of Scientific
Reports-A
E-ISSN: 2687-6167
Number 49, June 2022

REVIEW ARTICLE

PROTON TRANSFER SALTS and THEIR COMPLEXES and MIXED-LIGAND COMPLEXES of PYRIDINE DICARBOXYLIC ACIDS and PIPERAZINES: A SHORT REVIEW

Nurgün BÜYÜKKIDAN*

*Kütahya Dumlupınar University, Arts and Science Faculty, Chemistry Department, nurgun.buyukkidan@dpu.edu.tr, ORCID: 0000-0001-6879-9355

Receive Date:28.01.2022 *Accepted Date: 24.06.2022*

ABSTRACT

In this study, a short review covering the years 2009-2021 was made about the proton transfer salts obtained from the reaction of pyridine-acids, which are accepted as suitable proton donors, and piperazines, which are proton acceptors, and their metal complexes and mixed ligand metal complexes. In some complexes studied, both initial ion pairs bind to the metal, while in others they contain only one of the cationic and anionic moieties as ligands.

Keywords: *Proton transfer salt, Piperazine, Pyridine, Mixed ligand, Metal complexes*

1. INTRODUCTION

Heterocyclic compounds have a large range of uses in industry and various areas of chemistry [1]. Piperazine among heterocyclic rings containing nitrogen atoms has different application areas such as materials, agricultural chemicals and pharmaceutical chemistry. Studies have shown that piperazine and its derivatives have the following biological activities: anti-fungal [2], anti-depressant [3], anti-malarial [4], anti-migraine [5], anti-diabetic [6], anti-aggregating [7], anti-tumor [8, 9], anti-inflammatory [10], anti-obesity [11], and cardio-vascular [12]. As piperazine derivatives have many biological applications, there is an increasing interest in the synthesis of these compounds. In recent years, reaction mechanisms based on the proton transfer system were used in the preparation of metal complexes [13-15]. The very different geometries of the complexes are due to the coordinated covalent bonds between metals (transition, lanthanide and main group) and ligands. Supramolecular metal compounds, called metal-organic frameworks (MOF) [16], can be obtained from the formation of supramolecular proton transfer salts from a good proton donor-acceptor system and their reaction with s, p, d block and even f block metals. Supramolecular structures contain intramolecular or intermolecular interactions as O–H···O, O–H···N, N–H···O, N–H···N [17-19]. Pyridine carboxylic acids, which are found in natural products like alkaloids, coenzymes and vitamins, have great importance in medicinal chemistry due to their various physiological properties [20]. It has been reported that pyridine-2,4-dicarboxylic acid protects certain enzymes from heat inactivation [21], while 2,5- and 2,6-pyridinedicarboxylic acids activate or inhibit certain metalloenzymes [22, 23]. Pyridine dicarboxylates are among the most versatile ligands known, containing different functional groups that can coordinate to metal atoms.

This study aims to describe the reactions of piperazine and its derivatives with pyridine-di carboxylic acids, the synthesis of their metal complexes and their spectral and structural properties. In this work, proton transfer salts and their complexes and mixed ligand complexes obtained from piperazines and pyridine-dicarboxylic acids between 2009-2021 are presented. The pyridine-dicarboxylic acids for proton donors are: pyridine-2,3-dicarboxylic acid (Py-2,3-H_2Dc), pyridine-2,5-dicarboxylic acid (Py-2,5-H_2Dc) and pyridine-2,6-dicarboxylic acid (Py-2,6-H_2Dc). Bases used as proton acceptors are: Piperazine (Ppz), 2-(piperazin-1-yl)ethanol (HOEtPpz) and 2-piperazin-1-yl-ethanamine (PpzEa).

2. SYNTHESIS

The metal complexes reported in this study were synthesized either from the proton transfer salt formed by pyridine dicarboxylic acids and piperazines, or from mixed-ligands under hydrothermal conditions.

2.1. Proton Transfer Reaction

The reaction or reaction mechanism in which a proton (H^+) is separated from one species such as an acid and accepted by another species such as a base is called a proton transfer reaction. The stability of proton transfer types relies on many agents, such as the attractive and repulsive forces of opposite charges, the nature of the solvent, the geometry and topology of the acid and base. In the preparation of an effective ion pair that forms the components of the proton transfer salt and accelerates the formation of the metal complex, it may be useful to consider the following aspects [24-26]. i. Selection of functional acids and bases that can act as polydentate ligands in the formation of complexes, ii. Selection of donors and acceptors sensitive to intermolecular H-bonding and π-π stacking, iii. Selection of convenient acceptors and donors, taking into account the acidity and basicity constants, to ensure exact H-transfer. Proton transfer salts and their metal compound are of biological interest to chemists [27, 28].

2.2. Hydrothermal Synthesis

The synthesis of substances in a closed heated solution above ambient pressure and temperature is called hydrothermal synthesis. Hydrothermal method, which is a liquid phase preparation technology, has been developing rapidly in recent years [29]. It includes the development of new synthetical methods and techniques for the preparation of new materials. Hydrothermal technology is used in many branches of science such as earth science, materials science, physics, metallurgy, biology and chemistry [30-33]. Hydrothermal *in situ* ligand synthesis, such as hydrolation or decarboxylation of carboxyl groups, has become a very important method in the synthesis of organic ligands and their metal complexes, and in coordination engineering. This method is very useful for the synthesis of MOFs that are difficult to obtain at room conditions. Many coordination polymers synthesized by this method have been reported in the literature [16-19, 34-36].

2.3. Pyridine-dicarboxylic Acids

The isomers of pyridine-dicarboxylic acid (2,3-, 2,4-, 2,5-, 2,6-, 3,4- and 3,5-dicarboxylic acid) (Figure 1) have different coordination patterns with transition metals [37,38], main group elements [39, 40], and inner transition elements [41-43].

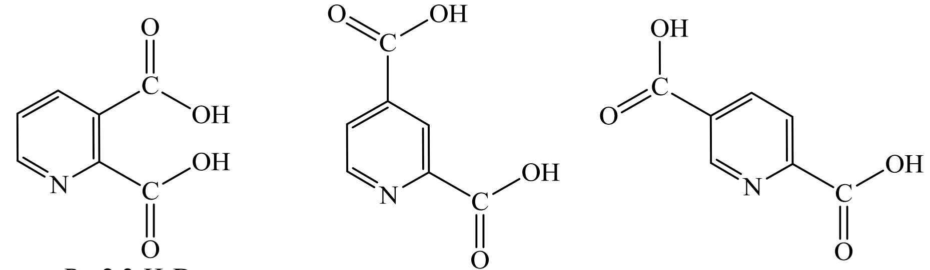

a. Py-2,3-H_2Dc **b.** Py-2,4-H_2Dc **c.** Py-2,5-H_2Dc

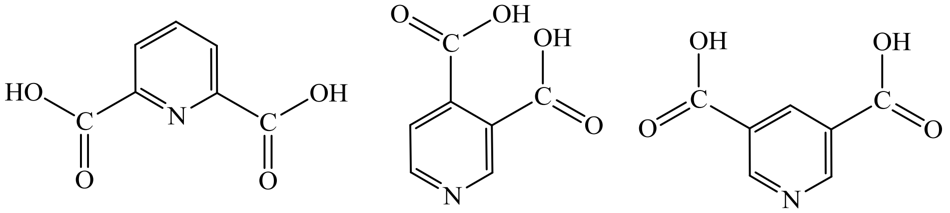

d. Py-2,6-H_2Dc **e.** Py-3,4-H_2Dc **f.** Py-3,5-H_2Dc

Figure 1. Isomers of pyridine-dicarboxylic acid.

2.3.1. Pyridine-2,3-dicarboxylic acid (Py-2,3-H_2Dc)

Py-2,3-H_2Dc (Figure 1a) can be highly neurotoxin and cell death may occur as a result of overstimulation of nerve cells. Brain toxicity caused by quinolinic acid has been associated with diseases such as autism, depression, dementia, stroke, Alzheimer's, and schizophrenia [44]. Different coordination modes of Py-2,3-HDc^- and Py-2,3-Dc^{2-} anions with various metal ions have been reported in the literature. The presence of versatile and different coordination motifs of Py-2,3- H_2Dc is quite remarkable in the construction of polymeric structures [45]. The different binding modes of the Py-2,3-Dc^{2-} ion allow it to act as a monodentate, tridentate, tetradentate, and quintuple ligand [46, 47] (Figure 2).

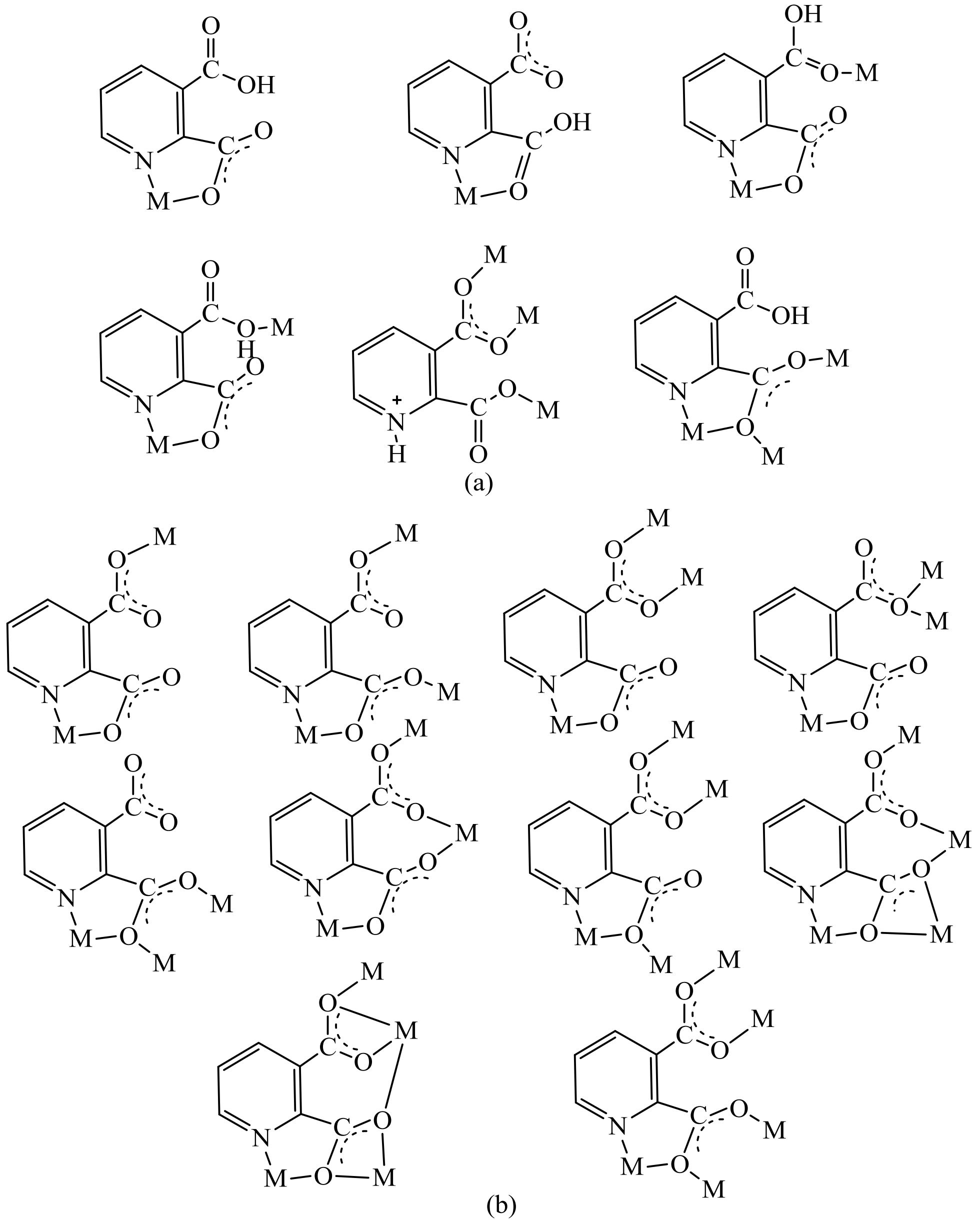

Figure 2. Coordination forms of (a) Py-2,3-HDc$^-$ anion (b) Py-2,3-H$_2$Dc^{2-} anion.

2.3.1.1. Proton transfer salt, $(H_2Ppz)^{2+}$(Py-2,3-HDc)$_2^-$ (1) and its metal complexes 2 and 3

The proton transfer salt **1** (Figure 3), $(H_2Ppz)^{2+}$(Py-2,3-Dc)$_2^-$, was prepared from the Py-2,3-H$_2$Dc and Ppz [48].

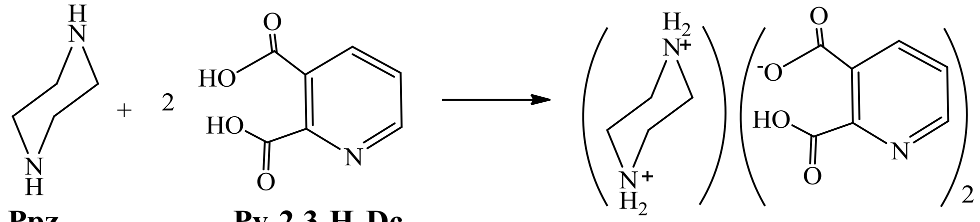

Figure 3. Synthesis of $(H_2Ppz)^{2+}(Py\text{-}2,3\text{-}HDc)_2^-$ (**1**).

The fact that Py-2,3-H_2Dc has variable and different coordination motifs makes it interesting in terms of forming polymeric architecture. Polymeric MOF compounds $\{(H_2Ppz)[Mn(Py\text{-}2,3\text{-}Dc)_2]\cdot 7.75H_2O\}_n$ (**2**), and $\{(H_2Ppz)[Hg_4Cl_{10}]\}_n$ (**3**) [49] (Figure 4) were obtained from the proton transfer salt, $(H_2Ppz)(Py\text{-}2,3\text{-}HDc)_2$ (**1**), with corresponding metal salts. The analyses, space groups and crystal systems of the compounds **1-4** are given in Table 1.

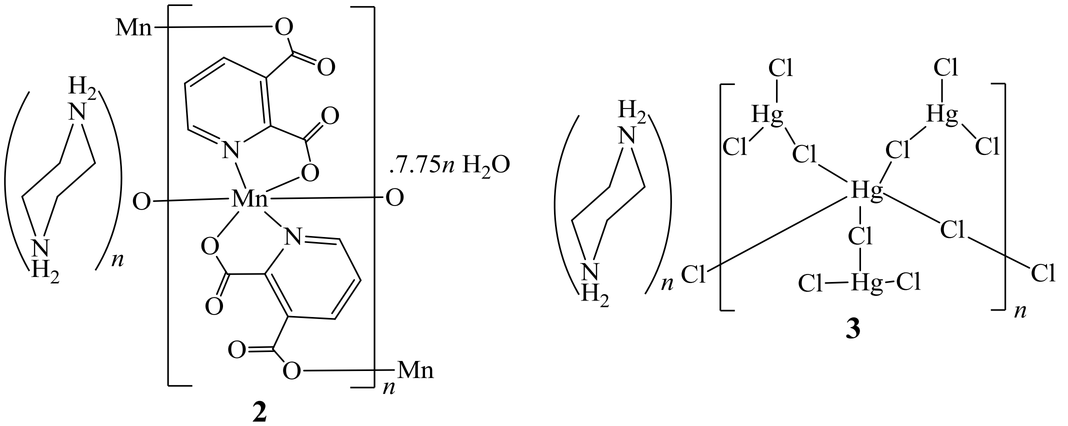

Figure 4. The structures of compounds **2** and **3.**

Table 1. The analyses, space groups and crystal systems of the compounds **1-4.**

Ref. No	Analyses	Proton Transfer Salts and Complexes	Space Group	Crystal system
48	X-ray	$(H_2Ppz)^{2+}(Py\text{-}2,3\text{-}HDc)_2^-$ (**1**)	$P2_1/c$	Monoclinic
49	NMR, IR and X-ray	$\{(H_2Ppz)[Mn(Py\text{-}2,3\text{-}Dc)_2]\cdot 7.75H_2O\}_n$ (**2**)	$P2_1/c$	Monoclinic
49	NMR, IR and X-ray	$\{(H_2Ppz)[Hg_4Cl_{10}]\}_n$ (**3**)	$C2/c$	Monoclinic
52	X-ray	$(H_2Ppz)^{2+}(Py\text{-}2,3\text{-}Dc)^{2-}\cdot CH_3OH$ (**4**)	$P2_1/n$	Monoclinic

The molecular structure of the Mn(II) (**2**) complex (Figure A1) includes two distinct Mn^{2+} ions, each located at the middle of a parallel 1-D chain. One of the Mn^{2+} ions (Mn1) binds to the O1, N1, O5 and N2 atoms of the two Py-2,3-Dc^{2-} ligands and to the O4 and O8 atoms of the other two Py-2,3-Dc^{2-} ligands, forming the six-coordinated structure. The other Mn^{2+} ion (Mn2) binds to the O9, N3, O13 and N4 atoms of the two Py-2,3-Dc^{2-} ligands and to the O12 and O16 atoms of the other two Py-2,3-Dc^{2-} ligands to form the six coordinated structure. The bond angles of O1–Mn1–O5 and O9–Mn2–O13 are 164.9 (1)° and 163.8 (1)°, respectively. These values show that the bond angles around both Mn^{2+} ions deviate from linearity and have a distorted octahedral geometry. When the Hg(II) (**3**) compound is compared with the Zn(II) [50] and Cd(II) [51] complexes, it is seen that it has a different structure. In the Zn(II) compound, two Py-2,3-Dc^{2-} ligands are coordinated to the metal, while H_2Ppz^{2+} remains as a complementary ion. The Cd^{2+} ion is coordinated by three aqua and a Py-2,3-Dc^{2-} ligand, while the H_2Ppz^{2+} cation is absent in the structure. It was found that the Hg(II) (**3**) compound, in which an endless network of chlorine and mercury atoms balanced with H_2Ppz^{2+}cation fragments, has a different structure compared to **2**, Zn(II) and Cd(II) (Figure 5).

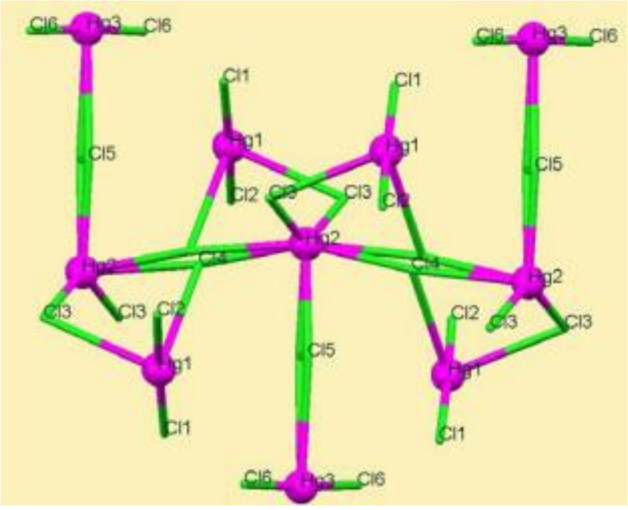

Figure 5. Coordination medium of Hg^{2+} ions in the Hg-Cl network of $\{(H_2Ppz)[Hg_4Cl_{10}]\}_n$ (**3**), H_2Ppz^{2+} is omitted.

2.3.1.2. Proton transfer salt $(H_2Ppz)^{2+}(Py\text{-}2,3\text{-}Dc)^{2-}$. CH_3OH (4)

The moieties in the proton transfer salt, $(H_2Ppz)^{2+}(Py\text{-}2,3\text{-}Dc)^{2-}\cdot CH_3OH$ (**4**) [52] (Figure 6) obtained from the reaction of Ppz and Py-2,3-H_2Dc in methanol form the 3-D structure by connecting with H-bonds O–H···O, N–H···O and C–H···O. The asymmetric unit of proton transfer salt (**4**) has one $(H_2Ppz)^{2+}$ cation, one (Py-2,3-Dc)$^{2-}$ anion and one CH_3OH with two H-bonds.

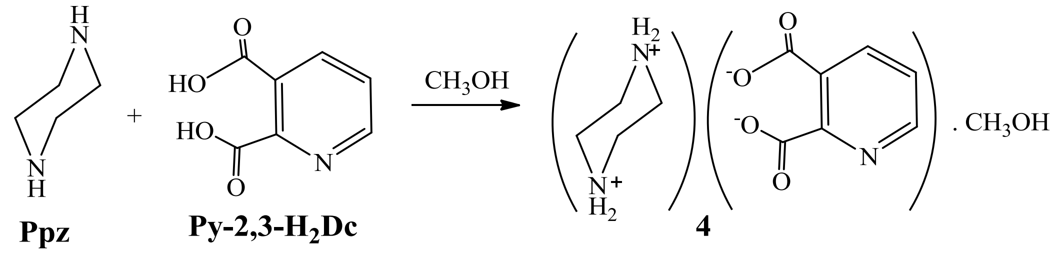

Figure 6. Synthesis of proton transfer salt, (H_2Ppz)(Py-2,3-Dc)·MeOH (**4**).

The C–O···π and C–H···π stackings are observed between the C6–O2 and N1/C1–C5 ring (3.5240 (9) Å) and between the C12–H1A and N1/C1–C5 ring (2,791 (1) Å) [52], respectively (Figure 7).

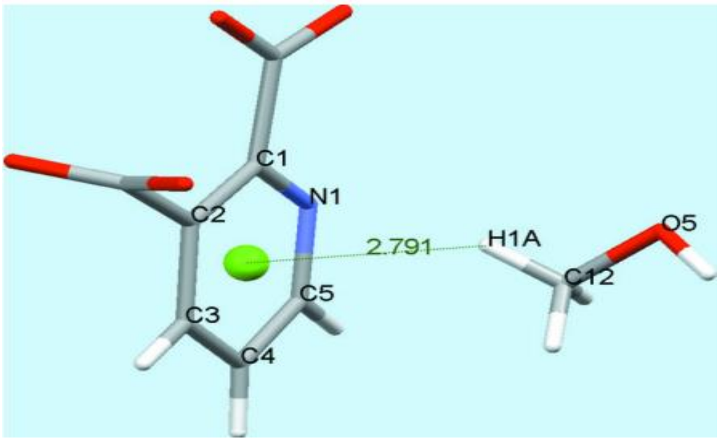

Figure 7. The C–H···π stacking of (**4**).

2.3.2. Pyridine-2,5-dicarboxylic acid (Py-2,5- H_2Dc) and it's complexes (5-13)

Py-2,5-H_2Dc (Figure 1c) is known as isosicomeronic acid. Py-2,5-HDc$^-$ and Py-2,5-Dc^{2-} anions are versatile ligands coordinated to transition metals with nitrogen and four oxygen atoms, and numerous polymeric complexes of these have been reported. [53-55]. The coordination forms of Py-2,5-H_2Dc are shown in Figure 8. It has been stated that derivatives of Py-2,5-H_2Dc show inhibitory effect against hepatitis B virus [56], and metal complexes have many applications such as enzyme inhibition [57], antibacterial activity [58], magnetism [59], catalysis [60], surface chemistry [61], aqueous solution chemistry [62]. Since 2009, proton transfer salts of Py-2,5-H_2Dc and metal complexes obtained from these salts have not been encountered. The complexes (**5-13**) of Py-2,5-H_2Dc in the literature are metal complexes obtained under hydrothermal conditions with mixed ligands. The analyses, space groups and crystal systems of the compounds **5-13** are given in Table 2.

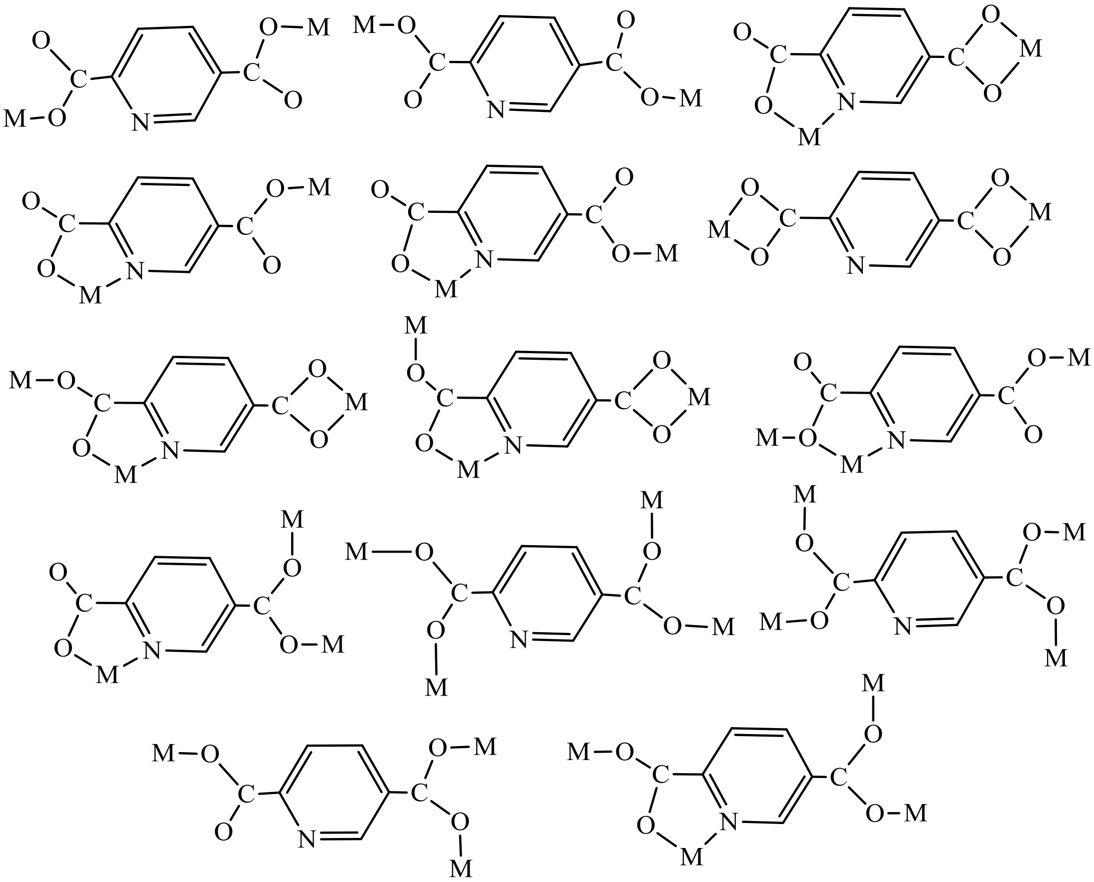

Figure 8. Coordination forms of Py-2,5-H_2Dc.

Table 2. The analyses, space groups and crystal systems of the mixed ligand complexes **5-13.**

Ref. No	Analyses	Complexes	Space Group	Crystal system
63	X-ray, UV, IR, TGA, Elemental analysis	[Co(Py-2,5-Dc)$_2$(H$_2$O)]·(Ppz)·2H$_2$O}$_n$ (**5**)	$P2_1/c$	Monoclinic
64	UV, SPS, X-ray	[Ni(Py-2,5-Dc)$_2$(HPpz)$_2$]·H$_2$O (**6**)	$C2/c$	Monoclinic
66	X-ray, PXRD, IR, TGA, FESEM, Elemental analysis	[Ce(Py-2,5-Dc)(Ppz)$_{1/2}$(H$_2$O)] (**7**)	$P2_1/c$	Monoclinic
66	X-ray, PXRD, IR, TGA, FESEM, Elemental analysis	[Pr(Py-2,5-Dc)(Ppz)$_{1/2}$(H$_2$O)] (**8**)	$P2_1/c$	Monoclinic
69	X-ray, PXRD, IR, UV, TGA and photoluminescence measurements	{(H$_2$Ppz)[Mn(Py-2,5-Dc)$_2$(H$_2$O)]·2H$_2$O} (**9**)	$P2_1/c$	Monoclinic

70	IR, PXRD, SEM, TGA and EDX elemental mapping analysis.	$\{(H_2Ppz)[Zn_{1/3}Fe_{2/3}(Py\text{-}2,5\text{-}Dc)_2(H_2O)]\cdot 2H_2O\}$ **(10)**	-	-
70	X-ray	$\{(H_2Ppz)[Fe(Py\text{-}2,5\text{-}Dc)_2(H_2O)]\cdot 2H_2O\}$ **(11)**	$P2_1/c$	Monoclinic
71	IR, PXRD, SEM, TGA and EDX elemental mapping analysis.	$\{(H_2Ppz)[Co_{1/3}Fe_{2/3}(Py\text{-}2,5\text{-}Dc)_2(H_2O)]\cdot 2H_2O\}$ **(12)**	-	-
72	IR, PXRD, SEM, TGA and EDX elemental mapping analysis	$\{(H_2Ppz)[Zn_{1/3}Co_{2/3}(Py\text{-}2,5\text{-}Dc)_2(H_2O)]\cdot 2H_2O\}$ **(13)**	-	-

2.3.2.1. Mixed-ligand complex $[Co(Py\text{-}2,5\text{-}Dc)_2(H_2O)]\cdot(Ppz)\cdot 2H_2O\}_n$ (5)

The asymmetric unit of hidrothermally synthesized complex, $[Co(Py\text{-}2,5\text{-}Dc)_2(H_2O)]\cdot(Ppz)\cdot 2H_2O\}_n$ (**5**) [63], consists of a Co(II) cation, two $Py\text{-}2,5\text{-}Dc^{2-}$, an aqua ligand, two lattice water and an uncoordinated Ppz. The $Py\text{-}2,5\text{-}Dc^{2-}$ moieties bind to Co(II) ions in two different ways. In the first of these, the nitrogen atom of the $Py\text{-}2,5\text{-}Dc^{2-}$ and one oxygen atom of the neighboring carboxylate group coordinate to a Co(II) ion and the other carboxylate group to the other Co^{2+} ion. In the second, the neighboring carboxylate group and a nitrogen atom coordinate to a Co^{2+} ion, while the other carboxylate group does not participate in the coordination. In its crystal structure, initially, Co(II) ions bind to $Py\text{-}2,5\text{-}Dc^{2-}$ groups, forming a 1-D chain along the b-axis (Figure A2a). Next, the 1-D chains are linked by H-bonds between the coordinated H_2O molecules and the uncoordinated carboxylate oxygen atoms of the two $Py\text{-}2,5\text{-}Dc^{2-}$ rings along the c-axis and an H-bonded 2-D structure is created in the bc plane (Figure A2b).

2.3.2.2. Mixed-ligand complex $[Ni(Py\text{-}2,5\text{-}Dc)_2(HPpz)_2]\cdot H_2O$ (6)

The mononuclear $[Ni(Py\text{-}2,5\text{-}Dc)_2(HPpz)_2]\cdot H_2O$ (**6**) with six coordinated, distorted octahedral geometry, was hydrothermally obtained [64]. The compound contains a Ni^{2+} cation, two $Py\text{-}2,5\text{-}Dc^{2-}$ anions, two $HPpz^{2+}$ cations, and a lattice H_2O molecule (Figure A3). The Ni^{2+} cation was coordinated to O1, O1A, N1 and N1A atoms of two $Py\text{-}2,5\text{-}Dc^{2-}$ anions in equatorial plane and to N2 and N2A atoms of $HPpz^{+}$ cation in axial positions. Although the bond lengths of Ni–N (2.0398(14) and 2.2033(15) Å) and Ni–O (2.0664(13) Å) are slightly longer than those reported for Py-2,5-Dc-Ni complexes, they are still within normal limits [61]. The C–O bond lengths of the two $Py\text{-}2,5\text{-}Dc^{2-}$ ligands are 1.274(2), 1.234(2), 1.256(2) and 1.244(2) Å, indicating that the both carboxylic groups are deprotonated. In $HPpz^{+}$ fragment, one of the N-atoms coordinates to the Ni(II) ion, while the other N-atom is protonated and turns into NH^{2+} [65]. The compound forms a network within a 3-D supramolecule through intermolecular N–H···O H-bonds.

2.3.2.3. Mixed-ligand complexes $[Ce(Py\text{-}2,5\text{-}Dc)(Ppz)_{1/2}(H_2O)]$ (7) and $[Pr(Py\text{-}2,5\text{-}Dc)(Ppz)_{1/2}(H_2O]$ (8)

The solution of $Ln(NO_3)_3.6H_2O$, (Ln = Ce and Pr), $Py\text{-}2,5\text{-}H_2Dc$ and Ppz in H_2O (5 mL) with the molar ratio of 1:3:1 was heated at 160 °C. After 3 days the yellow $[Ce(Py\text{-}2,5\text{-}Dc)(Ppz)_{1/2}(H_2O)]$ (**7**) (Ppz = 2,5-piperazinedicarboxylic acid) and the green $[Pr(Py\text{-}2,5\text{-}Dc)(Ppz)_{1/2}(H_2O)]$ (**8**) complexes were obtained [66]. A ligand was synthesized in the presence of piperazine and pyridine-2,5-

dicarboxylic acid by hydrothermal *in situ* ligand synthesis method such as hydrolation or decarboxylation of carboxyl groups, where ligand synthesis is rarely observed [67, 68]. Both of the carboxyl groups of the Py-2,5-Dc^{2-} ligand were separated and bound to the 2- and 5-positions of the piperazine ring, producing 2,5-piperazinedicarboxylic acid. The coordination polymers **7** and **8** formed by bridging mixed ligands are isostructural have interesting 3-D frameworks. 3-D structure of **8** is shown in Figure A4. In complexes **7** and **8** the coordination number of both Pr and Ce atoms are nine. Each asymmetric unit of compounds (**7** and **8**) includes one metal ion, half of Ppz, one Py-2,5-Dc^{2-}, and one aqua ligand. The geometry of the Pr(III) and Ce(III) ions are monocapped square-antiprism [66].

2.3.2.4. Mixed-ligand complex {(H_2Ppz)[Mn(Py-2,5-Dc)$_2$(H_2O)]·2H_2O} (9)

Hidrothermally synthesized metal-organic coordination polymer {(H_2Ppz)[Mn(Py-2,5-Dc)$_2$(H_2O)]·2H_2O} (**9**) [69] is soluble in water. The asymmetric unit of the Mn(II) complex contains one Mn(II) ion, two Py-2,5-Dc^{2-} ligands, one H_2Ppz^{2+} cation, one water molecule, and two uncoordinated water molecules (Figure A5). The Mn^{2+} ion binds to both carboxylate oxygen atoms of one of the two Py-2,5-Dc^{2-} ligands, while it coordinates to only one carboxylate oxygen of the other Py-2,5-Dc^{2-} ligand. It also binds to one water molecule and the nitrogen atoms of both Py-2,5-Dc^{2-} ligands. Thus, there are a total of six coordinated groups around the Mn^{+2} ion. The avarege bond lengths of Mn–O and Mn–N are 2.17 and 2.25 Å, repectively. The bond angles of O–Mn–O/N–Mn–N are in the range 75.49(7)-172.89(7)°. H-bond interaction was formed between the hydrogens of the coordinated H_2O molecule (H1A and H1B) and the O(3) and O(8) atoms of the two Py-2,5-Dc^{2-} ligands. 2-D structures connected by two lattice water molecules and Ppz^{2+} cation *via* N–H···O and O–H···O H-bond interactions form a 3-D supramolecular structure [69].

2.3.2.5. Mixed-ligand complexes {(H_2Ppz)[$Zn_{1/3}Fe_{2/3}$(Py-2,5-Dc)$_2$(H_2O)]·2H_2O} (10), {(H_2Ppz)[Fe(Py-2,5-Dc)$_2$(H_2O)]·2H_2O} (11), {(H_2Ppz)[$Co_{1/3}Fe_{2/3}$(Py-2,5-Dc)$_2$(H_2O)]·2H_2O} (12) and {(H_2Ppz)[$Zn_{1/3}Co_{2/3}$(Py-2,5-Dc)$_2$ (H_2O)]·2H_2O} (13)

The isostructural Fe compound, {(H_2Ppz)[Fe(Py-2,5-Dc)$_2$(H_2O)]·2H_2O} (**11**), with hydrothermally obtained mixed metal coordination polymers {(H_2Ppz)[$Zn_{1/3}Fe_{2/3}$(Py-2,5-Dc)$_2$(H_2O)]·2H_2O} [70] (**10**) and {(H_2Ppz)[$Co_{1/3}Fe_{2/3}$(Py-2,5-Dc)$_2$(H_2O)]·2H_2O} [71] (**12**) was synthesized to confirm the structures of these mixed metal compounds (**10** and **12**). Heterobimetallic coordination polymer (**12**) has been used as the sole source precursor for the synthesis of nano-sized $CoFe_2O_4$ by thermal decomposition [71]. Also, to confirm the structure of MOF compound, {(H_2Ppz)[$Zn_{1/3}Co_{2/3}$(Py-2,5-Dc)$_2$ (H_2O)]·2H_2O} (**13**) [72], the isostructural Co complex {(H_2Ppz)[Co(Py-2,5-Dc)$_2$(H_2O)]·2H_2O} (**5**) [63] was used. Decomposition of **13** at 400 °C results in nano-size $ZnCo_2O_4$ [72].

2.3.3. Pyridine 2,6-dicarboxylic acid (Py-2,6-H_2Dc)

Py-2,6-H_2Dc (Figure 1d) which coordinates to the metal with N and O donor atoms and is known as dipicolinic acid, is a pyridine dicarboxylic acid that has been extensively studied because of its various coordination motifs. Py-2,6-H_2Dc and Ppz form a good binary system as proton donor-acceptor. Many ion pairs were reported from the reaction of Py-2,6-H_2Dc with different amines [73-75] and piperazines with different acids [48, 76, 77]. The coordination chemistry of Py-2,6-H_2Dc attracts more attention because it is a convenient ligand for the preperation of pharmacologically active compounds due to its low toxicity, different biological properties and amphiphilic nature [78,79]. It has been reported that metal ions have stronger interaction with target molecules and show more antimicrobial activity than free ligand [80]. Py-2,6-H_2Dc has a wide variety of coordination modes [81, 82] and it can coordinate to metal as a monodentate, bidentate, tridentate and bridging ligand as shown in Figure 9.

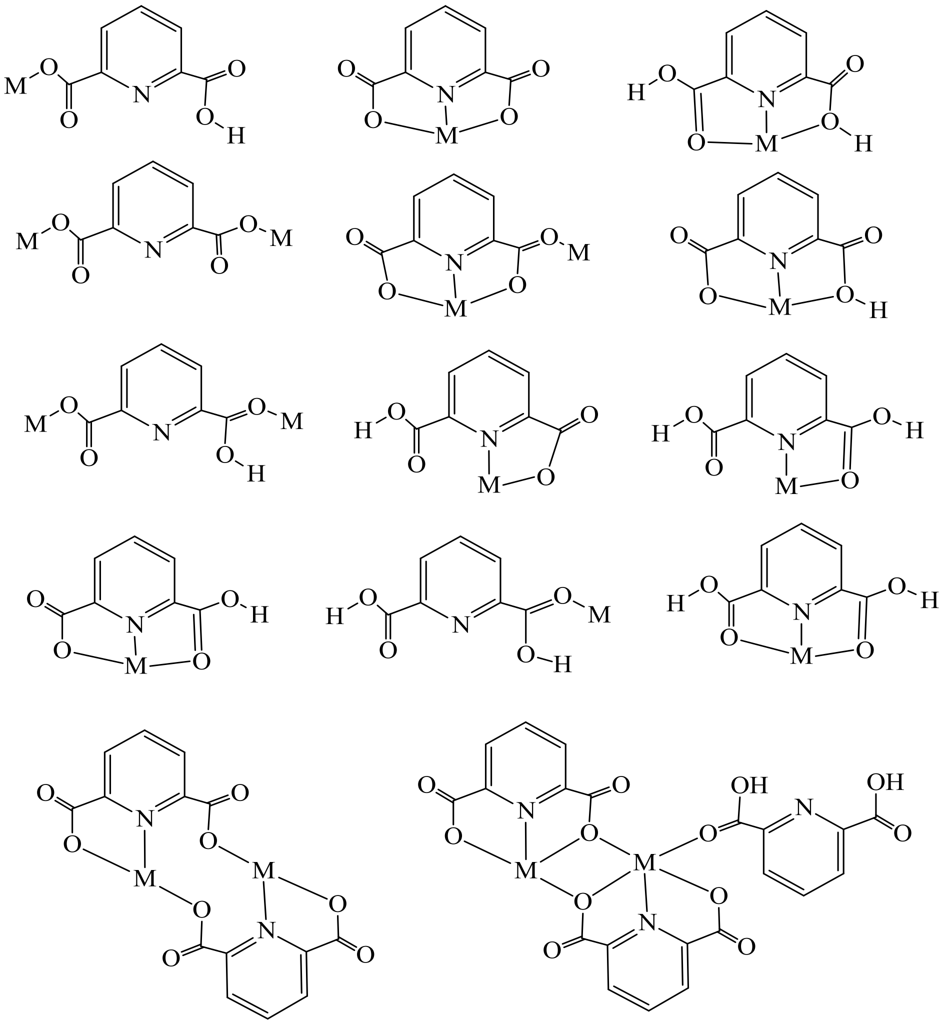

Figure 9. Versatile coordination forms of Py-2,6-H_2Dc.

2.3.3.1. Proton transfer salts and metal complexes

The analyses, space groups and crystal systems of proton transfer salts (**14**, **17** and **22)** and their metal complexes (**15** and **16**, **18-21** and **23-26)** are given in Table 3.

Table 3. The analyses, space groups and crystal systems of **14-26**.

Ref. No	**Analyses**	**Proton Transfer Salts and Complexes**	**Space Group**	**Crystal system**

83	X-ray, NMR, IR, and elemental analysis	$(H_2Ppz)(\ Py\text{-}2,6\text{-}Dc)$ (**14**)	*Pbcn*	Orthorhombic
84	X-ray, NMR, IR, and elemental analysis	$(H_2Ppz)[Cd(pydc)_2]\cdot 6H_2O$ (**15**)	*P1*	Triclinic
87	X-ray, NMR, IR, and elemental analysis	$(H_2Ppz)[Sb_2(Py\text{-}2,6\text{-}Dc)_4]\cdot 2H_2O$ (**16**)	*P1*	Triclinic
89	X-ray and elemental analysis	$(H_2Ppz)_{1.5}(Py\text{-}2,6\text{-}Dc\ H)_3\cdot 3.7H_2O$ (**17**)	*C2/c*	Monoclinic
89	X-ray, NMR, IR, and elemental analys	$(H_2Ppz)[Zr(Py\text{-}2,6\text{-}Dc)_3]\cdot 8H_2O$ (**18**)	*P1*	Triclinic
89	X-ray, NMR, IR, and elemental analys	$(H_2Ppz)[Ce(Py\text{-}2,6\text{-}Dc)_3]\cdot 8H_2O$ (**19**)	*P1*	Triclinic
91	X-ray, IR and elemental analysis	$(H_2Ppz)[Sr(Py\text{-}2,6\text{-}Dc)_2(H_2O)_2]n\text{-}\cdot 4H_2O$ (**20**)	$P2_1/n$	Monoclinic
91	X-ray, IR and elemental analysis	$[Ce(Py\text{-}2,6\text{-}Dc)_2(H_2O)_2]n\cdot 4H_2O$ (**21**)	$P2_1/c$	Monoclinic
97	NMR, IR and UV-Vis and elemental analysis	$(HOEtH_2Ppz)^{2+}(Py\text{-}2,6\text{-}HDc)_2^{-}$ (**22**)	-	-
97	X-ray, NMR, IR and UV-Vis, TG and elemental analyses	$(H_2Ppz)[Cu(Py\text{-}2,6\text{-}Dc)_2]\cdot 6H_2O$ (**23**)	$P2_1/c$	Monoclinic
98	X-ray, NMR, IR and UV-Vis, TG and elemental analyses	$(H_2Ppz)[Co(Py\text{-}2,6\text{-}Dc)_2]\cdot 6H_2O$ (**24**)	$P2_1/c$	Monoclinic
98	X-ray, NMR, IR and UV-Vis, TG and elemental analyses	$(H_2Ppz)[Ni(Py\text{-}2,6\text{-}Dc)_2]\cdot 6H_2O$ (**25**)	$P2_1/c$	Monoclinic
98	X-ray, NMR, IR and UV-Vis, TG and elemental analyses	$(H_2Ppz)[Zn(Py\text{-}2,6\text{-}Dc)_2]\cdot 6H_2O$ (**26**)	$P2_1/c$	Monoclinic

2.3.3.1.1. Proton transfer salt $(H_2Ppz)^{2+}(Py\text{-}2,6\text{-}Dc)^{2-}$ (14) and metal complexes 15 and 16

The proton transfer salt **14** reported in the literature was obtained [83] from a 1:1 molar ratio of a mixture of Py-2,6-H_2Dc and piperazine in THF (Figure 10).

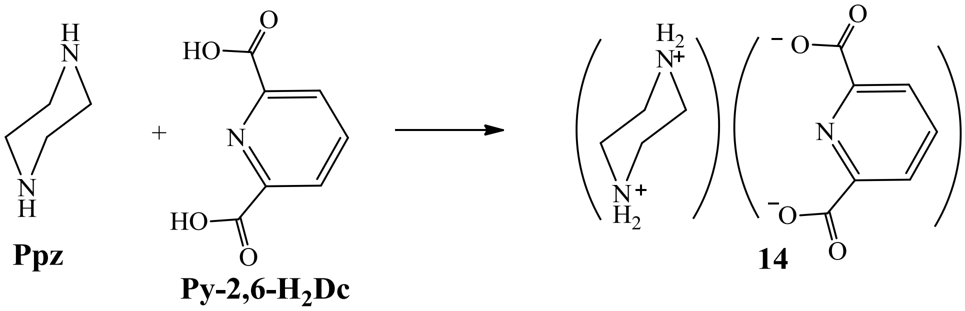

Figure 10. Synthesis of compound **14.**

The compound $(H_2Ppz)[Cd(Py\text{-}2,6\text{-}Dc)_2]\cdot 6H_2O$ (**15**) [84] (Figure 11) was synthesized from the proton transfer salt (**14**) [83] .

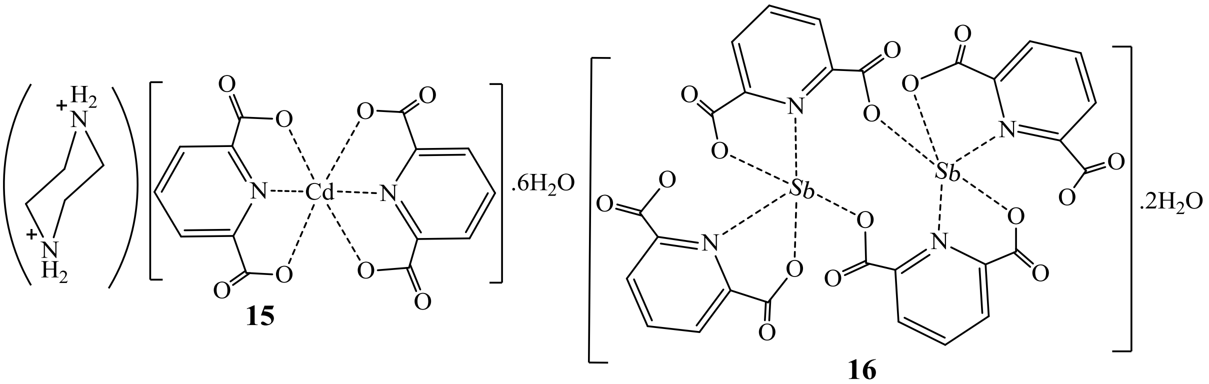

15

16

Figure 11. Structures of **15** and **16.**

In this complex, there are six uncoordinated water molecules that form hydrogen bonds with both $(H_2Ppz)^{2+}$ and $[Cd(Py\text{-}2,6\text{-}Dc)_2]^{2-}$ ions with a piperazinium ion as the counter ion. Complexes of metal ions Zn(II) [85] and Hg(II) [86], which are in the same group as Cd(II), obtained from the same proton transfer salt $(H_2Ppz)^{2+}(Py\text{-}2,6\text{-}Dc)^{2-}$ (**14**) have the same coordination environment. An increase in the order of Hg(II) > Cd(II) > Zn(II) was observed when the M–O bond lengths of the compounds were compared. It was found that the M–N bond in the Zn(II) complex was shorter than the others, but the Hg–N bond was also unexpectedly shorter than the Cd–N bond. In the anionic part of the complex, the N1'–Cd1–N1 angle was measured as 174.05(5) Å and it was observed that it deviated from linearity. It is understood that the two $(Py\text{-}2,6\text{-}Dc)^{2-}$ rings are not perpendicular to each other since the torsion angles of O3'–Cd–O3–C7 and O3'–Cd–O2–C6 are 105.52(9)° and 96.32(9)°, respectively. These data showed that the geometry of the complex is distorted octahedral around the six-coordinate Cd(II) ion (Figure 12).

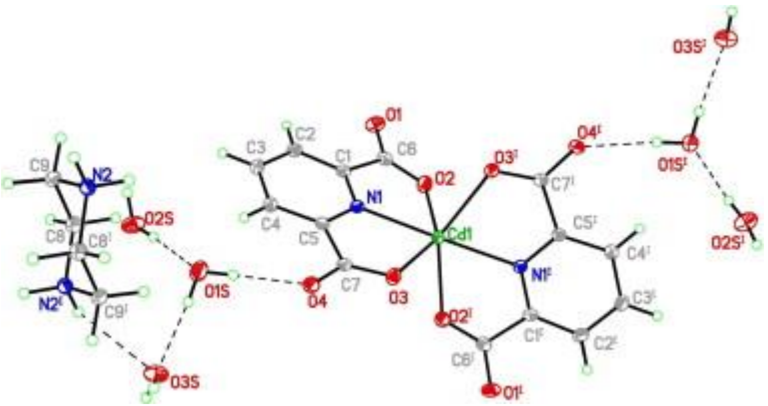

Figure 12. Molecular structure of $(H_2Ppz)[Cd(Py\text{-}2,6\text{-}Dc)_2]\cdot 6H_2O$ (**15**).

The compound (H_2Ppz)[Sb_2(Py-2,6-Dc)$_4$]·$2H_2O$ (**16**) [87] (Figure 11) was synthesized by the reaction of proton transfer compound **14** with the related metal salt. The ^{1}H NMR spectrum of (H_2Ppz)[Sb_2(Py-2,6-Dc)$_4$]·$2H_2O$ (**16**) exhibits two sets of peaks: signals at 3.33 ppm and at 8.42-8.25 ppm were attributed to the protons of (H_2Ppz)$^{2+}$ and (Py-2,6-Dc)$^{2-}$ moieties, respectively. Two of the four Py-2,6-Dc^{2-} anions in the binuclear Sb(III) complex bind to a metal center as tridentate and the other two as bidentate ligands to the other metal center. The angle between the N1/C2–C6 and N2/C9–C13 rings is 86.56°, indicating that the two Py-2,6-Dc^{2-} groups attached to the each metal center are nearly perpendicular to each other. From the crystallographic data, it is seen that the Sb1–N1(2.393(3) Å) and Sb1–O3A (2.464(3) Å) bonds are longer than the others (2.088(2)-2.282(3) Å). The bond angles around the Sb(III) ion show the distorted trigonal bipyramid in which the O1 and O3 atoms lie in the axial position. Compared with the similar complex of Bi(III) ion, {(H_2Ppz)[Bi_2(Py-2,6-Dc)$_4$(H_2O)]·H_2O}$_n$, which is in the same group as Sb(III), it was determined that Sb–N bond lengths were slightly shorter than Bi–N bond lengths, and Sb–O bond lengths were longer than Bi–O [88].

2.3.3.1.2. Proton transfer salt (H_2Ppz)$_{1.5}$(Py-2,6-HDc)$_3$·$3.7H_2O$, (17) and it's complexes 18-21

Pale yellow proton transfer salt **17**, (H_2Ppz)$_{1.5}$(Py-2,6-HDc)$_3$·$3.7H_2O$, was synthesized by the reaction of Py-2,6-H_2Dc and Ppz in THF [89] (Figure 13).

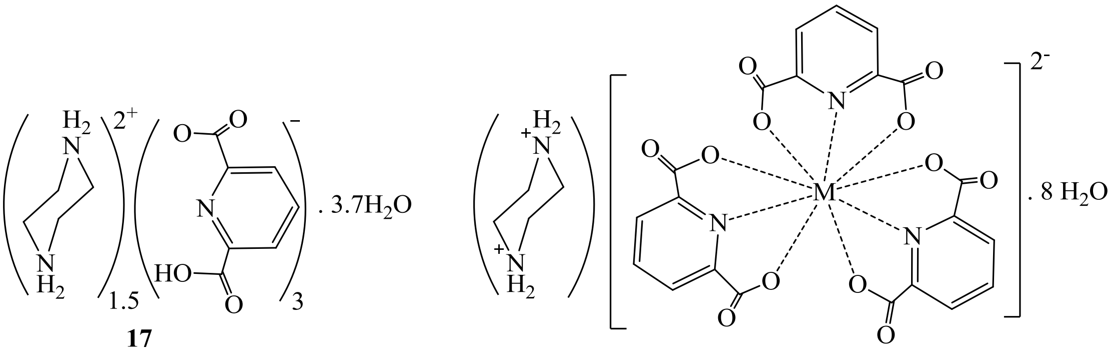

17

M = Zr(IV) (**18**) and Ce(IV) (**19**)

Figure 13. Proton transfer salt **17** and it's complexes **18** and **19.**

Only one of the hydrogens of the carboxylic acid was removed in complex **17**. The asymmetric units of the proton transfer salt **17** have three Py-2,6-Dc^{2-} rings and one and a half H_2Ppz ions to balance the charge. The strongest H-bond was observed as O1C–H1C···O3B (2.4700(14)Å) in the crystal structure of proton transfer salt **17**. In the molecular structure of **17**, π–π stacking was also observed as an intermolecular interaction between aromatic rings with the distance of 3.669(8) Å (Figure A6). The nine coordinated complexes Zr(IV) (**18**) and Ce(IV) (**19**) (Figure 13) were synthesized from the proton transfer salt **17** [89]. The asymmetric unit of complexes (H_2Ppz)[Zr(Py-2,6-Dc)$_3$]·$8H_2O$ (**18**) and (H_2Ppz)[Ce(Py-2,6-Dc)$_3$]·$8H_2O$ (**19**) contains three Py-2,6-Dc^{2-} ions as tridentate ligands, one H_2Ppz^{2+} and eight-uncoordinated H_2O. The Zr(IV) and Ce(IV) ions in each complex bind to the three N and six O atoms of the three Py-2,6-Dc^{2-} ligands [89]. In the molecular structure of **18** (Figure 14) the Zr–O (O1, O3, O5, O7, O9, O11) bond lengths are very close to each other and the Zr–N bond lengths are almost equal. The sum of the N1–Zr–N2, N2–Zr–N3 and N3–Zr–N1 bond angles is 360.00(8)°, indicating that the Zr(IV) ion is in the center of the N1–N2–N3 plane. When the crystal structure of **18** is compared with $(HPyDa)_2[Zr(Py\text{-}2,6\text{-}Dc)_3]\cdot 5H_2O$ (PyDa = pyridine-2,6-diamine) [90], it is seen that the bond lengths and bond angles surrounding the Zr(IV) ion are similar in both complexes. In the crystal structure of **18**, inter and intramolecular N–H···O, O–H···O, and C–H···O H-bonds have values ranging from 2.718(3) to 3.464(4) Å.

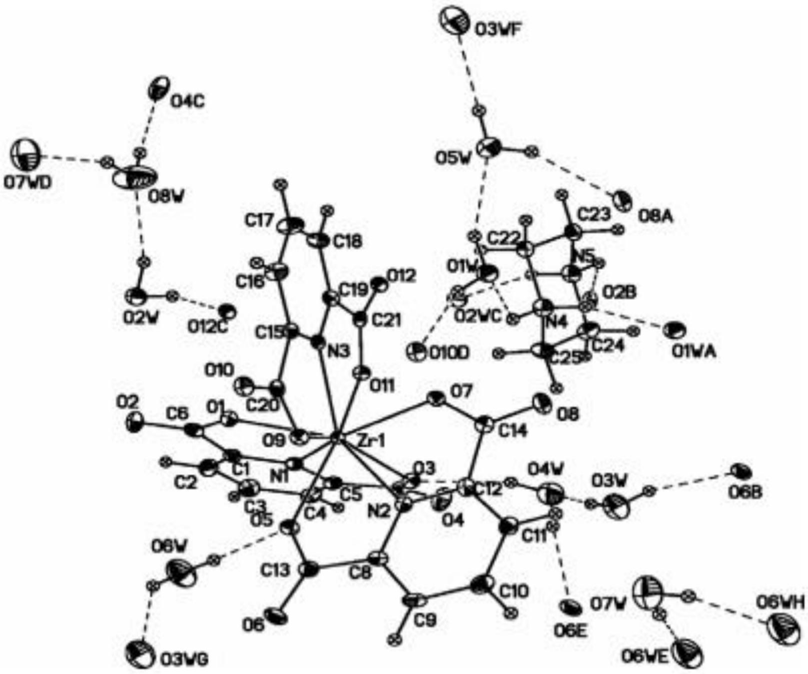

Figure 14. Molecular structure of **18**.

The geometry of $(H_2Ppz)[Ce(Py\text{-}2,6\text{-}Dc)_3]\cdot 8H_2O$ **(19)** is a distorted three-headed triangular prism with six oxygen atoms and three caps on its faces. The Ce(IV) complex has intramolecular and intermolecular H-bonds in its crystal structure, N–H···O, O–H···O, and C–H···O, with values ranging from 2.711(5) to 3.448(5) Å [89]. Complexes $(H_2Ppz)[Sr(Py\text{-}2,6\text{-}Dc)_2(H_2O)_2]n\cdot 4H_2O$ (**20**) and $[Ce(Py\text{-}2,6\text{-}Dc)_2(H_2O)_2]_n\cdot 4H_2O$ (**21**) were obtained [91] from the proton transfer salt **17** [89]. These complexes show characteristic bands in their IR spectra. The bands observed in the range of 3600–3200 cm^{-1} belong to the C–H, N–H and O–H stretching vibrations originating from the piperazine cation, pyridine-2,6-dicarboxylate and lattice water molecules [92]. Asymmetrical and symmetrical carboxylate vibrations were observed at 1680-1700 cm^{-1} and 1580 cm^{-1}, respectively. A Δv value of 120 cm^{-1} for complexes **20** and **21** indicates polybinding of the carboxylate to the metal [93]. In Sr(II) compound, the Sr(II) ion is binded to one oxygen atom of the bridge $Py\text{-}2,6\text{-}Dc^{2-}$ ion, two water molecules, and four oxygens and two nitrogens of two pyridine-2,6-dicarboxylates [91]. Intermolecular H-bonds and Sr-Py-2,6-Dc-Sr distances of **20** are of great importance in the formation of its 2-D supramolecular structure. The chair-form piperazine cations are very good H-bond donors and also act as complementary ions [94-96]. The $[Ce(Py\text{-}2,6\text{-}Dc)_2(H_2O)_2]_n\cdot 4H_2O$ (**21**) complex has a 3-D polymeric structure. The Ce(IV) ion is coordinated to the four oxygens and two nitrogens of the two $Py\text{-}2,6\text{-}Dc^{2-}$ anion, two oxygen atoms of the two H_2O molecules, and the one oxygen atom of the

Py-2,6-Dc^{2-} ion [91] **(**Figure 15). Sr(II) and Ce(IV) ions both have a distorted tricapped trigonal prism geometry.

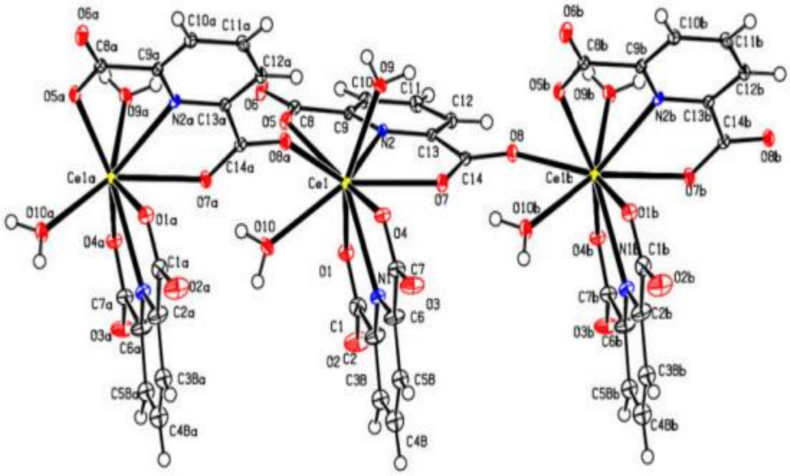

Figure 15. Polymeric structure of [Ce(Py-2,6-Dc)$_2$(H$_2$O)$_2$]n·4H$_2$O (**21**).

2.3.3.1.3. Proton transfer salt (HOEtH$_2$Ppz)$^{2+}$(Py-2,6-HDc)$_2^-$ (22) and it's complexes (23-26)

Proton transfer salt (HOEtH$_2$Ppz)$^{2+}$(Py-2,6-HDc)$_2^-$ (**22**) (HOEt H$_2$Ppz = 1-(2-hydroxyethyl)piperazine-1,4-dium) was obtained by the reaction of HOEtPpz and Py-2,6-H$_2$Dc [97] **(**Figure 16).

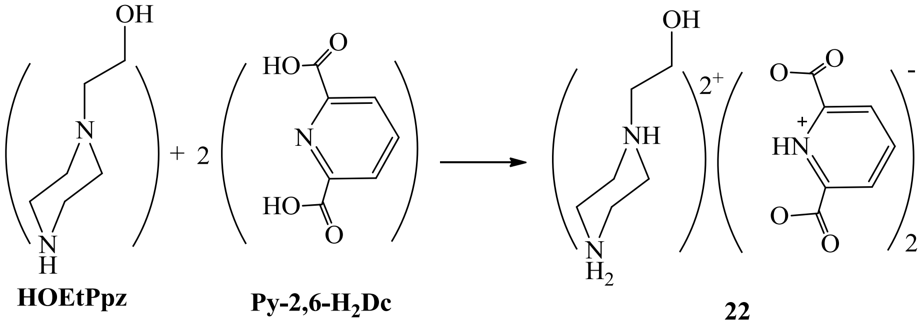

Figure 16. Synthesis of (HOEtH$_2$Ppz)$^{2+}$(Py-2,6-HDc)$_2^-$ (**22**).

^{1}H NMR spectrum of proton transfer salt (**22**) displayed signals at 3.35, 3.60 and 3.95 ppm for H$_2$HOEtPpz^{2+} and at 8.35 and 8.57 ppm for Py-2,6-HDc$^-$ fragments.

Complexes of proton transfer salt **22** (HOEtH$_2$Ppz)[M(Py-2,6-Dc)$_2$]·6H$_2$O (M = Cu(II) (**23**), Co(II) (**24**), Ni(II) (**25**) and Zn(II) (**26**)) consist of a HOEtH$_2$Ppz^{2+} cation as a complementary ion, two Py-2,6-Dc^{2-} anions as tridentate ligands and six uncoordinated water molecules (Figure 17) [97, 98].

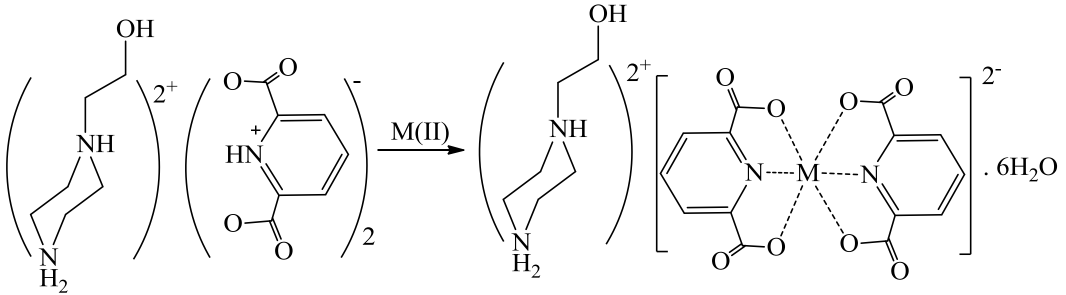

22

M = Cu(II) (**23**), Co(II) (**24**),
Ni(II) (**25**) and Zn(II) (**26**)

Figure 17. Synthesis of complexes **23-26**.

In crystal structure of Cu(II) (**23**) complex (Figure A7), O1–Cu–O4 and O7–Cu–O6 trans angles are low value as 156.3(3)° and 155.6(3)°, respectively. Despite, the N1–Cu–N2 trans angle is 174.0(3)°, closer to 180°. The dihedral angle between the planes of the two Py-2,6-Dc^{2-} rings is 87.1°, indicating that the two Py-2,6-Dc^{2-} ligands are perpendicular to each other [97]. Cu–N and Cu–O bond lengths of are in agreement with similar Cu(II) compounds [99,100]. The deviating from linearity bond angles around M(II) ions containing trans-donor atoms are 75.75(6)°-152.61(5)° for Co(II) (**24**), 77.73(5)°-156.39(5)° for Ni(II) (**25**) and 74.75(5)°-152.63(4)° for Zn(II) (**26**). These values indicate that the ideal octahedral geometry is distorted due to the binding of Py-2,6-Dc^{2-} ions to M(II) ions as tridentate ligands (Figure A7). M–N and M–O bonds are within normal ranges for complexes **24-26** [98].

2.3.3.2. Mixed ligand complexes (27-36) of Py-2,6-H_2Dc

The mixed ligand complexes (**27-36**) of Py-2,6-H_2Dc with various metals as p-, d- and f-blocks were synthesized. The analyses, space groups and crystal systems of mixed-ligand complexes (**27-36**) are given in Table 4.

Table 4. The analyses, space groups and crystal systems of mixed-ligand complexes **27-36.**

Ref. No	Analyses	Complexes	Space Group	Crystal system
101	X-ray	$[(H_2Ppz)[Co(Py\text{-}2,6\text{-}Dc)_2]\cdot 4H_2O$ (**27**)	$P2_1/n$	Monoclinic
103	X-ray, IR, NMR, UV-Vis, TGA and elemental analysis	$(HPpzEa)[Bi_2(Py\text{-}2,6\text{-}Dc)_3(HPy\text{-}2,6\text{-}Dc)(H_2O)_2]\cdot 5H_2O$ (**28**)	$P2_1/c$	Monoclinic
104	ICP, IR, TGA, X-ray, PXRD and elemental analysis	$(H_2Ppz)_n[Ce_2(Py\text{-}2,6\text{-}Dc)_4(H_2O)_2]n$ (**29**)	$P1$	Triclinic
104	ICP, IR, TGA, X-ray, PXRD and elemental analysis	$(H_2Ppz)_n[Pr_2\ (Py\text{-}2,6\text{-}Dc)_4(H_2O)_2]n$ (**30**)	$P1$	Triclinic
104	ICP, IR, TGA, X-ray, PXRD and elemental analysis	$(H_2Ppz)_n[Eu_2\ (Py\text{-}2,6\text{-}Dc)_4(H_2O)_2]n$ (**31**)	$P1$	Triclinic
105	ICP, IR, TGA, X-ray,	$(H_2Ppz)_n[Sm_2(Py\text{-}2,6\text{-}Dc)_4(H_2O)_2]_n$ (**32**)	$P1$	Triclinic

	PXRD and elemental analysis			
109	IR, TGA, X-ray, and elemental analysis	$(H_2Ppz)_3[Tb_2(Py\text{-}2,6\text{-}Dc)_6]\cdot 15H_2$ (**33**)	*P3*	
110	IR, TGA, X-ray, and elemental analysis	$(H_2Ppz)[Ce_2(Py\text{-}2,6\text{-}Dc)_4(H_2O)_4]\cdot H_2O$ (**34**)	*P1*	Triclinic
111	ICPOES, IR, TGA, X-ray, PXRD and elemental analysis	$(H_2Ppz)_n[La_2(Py\text{-}2,6\text{-}Dc)_4(H_2O)_2]_n$ (**35**)	*P1*	Triclinic
111	ICPOES, IR, TGA, X-ray, PXRD and elemental analysis	$(H_2Ppz)_n[Nd_2(Py\text{-}2,6\text{-}Dc)_4(H_2O)_2]_n$ (**36**)	*P1*	Triclinic

2.3.3.2.1. Mixed-ligand complex $[(H_2Ppz)[Co(Py\text{-}2,6\text{-}Dc)_2]\cdot 4H_2O$ (27)

After mixing the aqueous solution of $Co(NO_3)_2.6H_2O$ (2 mmol) and Py-2,6- H_2Dc (4 mmol) at room temperature for 45 minutes, an aqueous solution of piperazine (Ppz) (4 mmol) was added to this solution and the mixture was stirred for 4 h at 100 °C. The crystals of $[(H_2Ppz)[Co(Py\text{-}2,6\text{-}Dc)2]\cdot 4H_2O$ (**27**) were obtained by evaporation of the solution at room conditions [101]. In the Co(II) complex, the piperazindium cation was found to be in the chair conformation. The Co(II) ion, which has a distorted octahedral geometry, is coordinated to the two nitrogens and four oxygens of the two Py-2,6-Dc^{2-} rings (Figure 18).

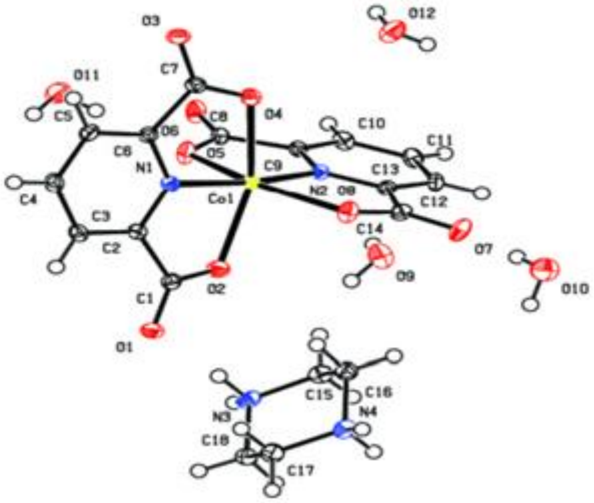

Figure 18. Molecular structure of $[(H_2Ppz)[Co(Py\text{-}2,6\text{-}Dc)_2]\cdot 4H_2O$ (**27**).

2.3.3.2.2. Mixed-ligand complex $(HPpzEa)[Bi_2(Py\text{-}2,6\text{-}Dc)_3(HPy\text{-}2,6\text{-}Dc)(H_2O)_2]\cdot 5H_2O$ (28)

Due to the large size of the Bi^{3+} ions, most Bi(III) compounds have a coordination number greater than six [102]. In dimeric complex $(HPpzEa)[Bi_2(Py\text{-}2,6\text{-}Dc)_3(HPy\text{-}2,6\text{-}Dc)(H_2O)_2]\cdot 5H_2O$ (**28**) (PpzEa = 2-piperazin-1-ylethanamine) Bi^{3+} has eight coordinated [103] (Figure 19).

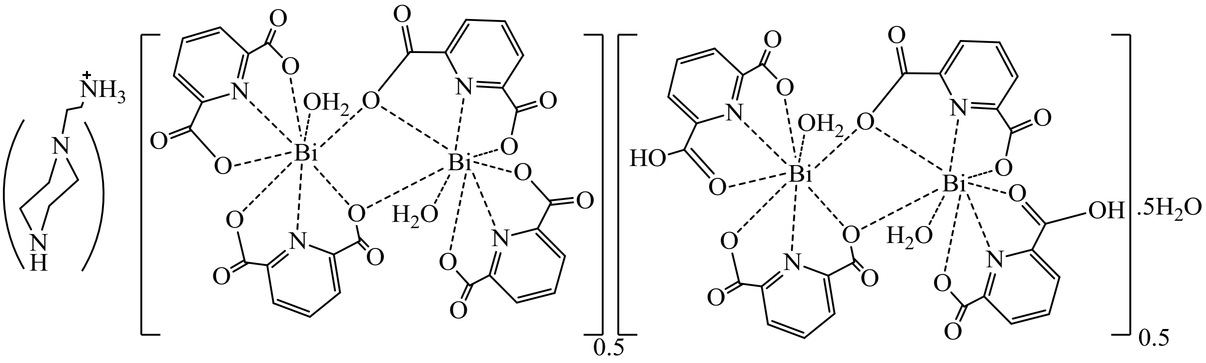

Figure 19. Structure of Bi(III) compound (**28**).

The asymmetric unit of **28** which obtained by hydrothermal method has two different bismuth ions, both Bi^{3+} cations bind to five oxygens and two nitrogens of three different Py-2,6-Dc $^{2-}$ anions and one oxygen of an aqua ligand.

2.3.3.2.3. Mixed-ligand complexes Ce(III) (29), Pr(III) (30) and Eu(III) (31)

Hydrothermally obtained three metal-organic frameworks containing lanthanide metals Ce(III) (**29**), Pr(III) (**30**) and Eu(III) (**31**), formulated as $(H_2Ppz)_n[Ln_2(Py\text{-}2,6\text{-}Dc)_4(H_2O)_2]_n$ are isomorphous [104]. The structures of complexes occur $[Ln_2(Py\text{-}2,6\text{-}Dc)_4(H_2O)_2]^{2-}$ anionic chains with $\{H_2Ppz\}^{2+}$ moiety occupying the interchain areas. The chains occur binuclear $[Ln_2(Py\text{-}2,6\text{-}Dc)_4(H_2O)_2]^{2-}$ structural constituents connected by *O*,*O'*-bridges of carboxylate fragments. In binuclear complexes, each of the lanthanide ions binds to five oxygens of the carboxylate groups of four Py-2,6-Dc^{2-} rings, two nitrogens, and two oxygens of the water ligands, forming a nine-coordinate structure.

2.3.3.2.4. Mixed-ligand complex $(H_2Ppz)_n[Sm_2(Py\text{-}2,6\text{-}Dc)_4(H_2O)_2]_n$ (32)

The asymmetric unit of the hidrothermally synthesized MOF complex $(H_2Ppz)_n[Sm_2(Py\text{-}2,6\text{-}Dc)_4(H_2O)_2]_n$ (**32**) contains the Sm(III) ion bonded to N and O atoms of the two Py-2,6-Dc^{2-} and the a H_2O ligand. It also contains half of the protonated piperazinium cation [105] (Figure 20a). The ladder structure in which pyridine-2,6-dicarboxylate is coordinated to the Sm(III) ion has been reported for the first time. The complementary piperazine cation is attached to the Sm(III) ladder by strong H-bonds. Also, there is an H-bond between one of the oxygens (O3) of the carboxylate groups and the coordinated water molecule (Figure 20b).

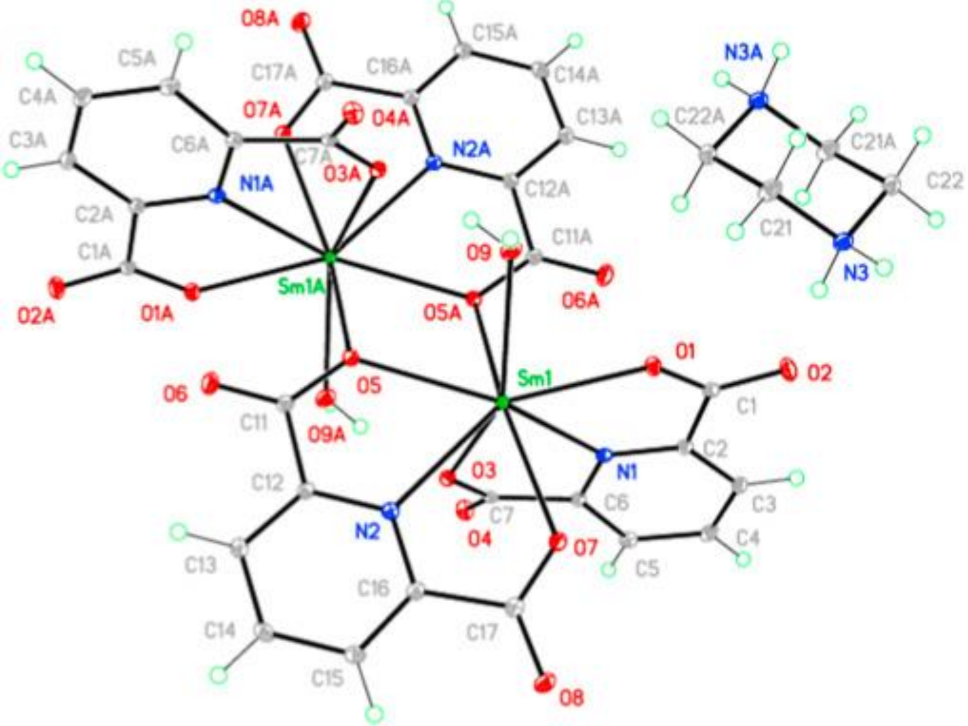
O8A
C15A
C5A
C17A
C16A
C14A
C4A
N3A
O7A
O4A
C13A
C22A
C3A
C6A
C7A
C21A
N1A
O3A
N2A
C22
C2A
C12A
C21
C11A
C1A
O9
N3
Sm1A
O6A
O2A
O1A
O5A
O1
O2
Sm1
C1
O6
O5
C11
O9A
C2
N1
C3
O3
C6
C12
C7
N2
O4
C4
O7
C5
C13
C16
C14
C17
C15
O8

(a)

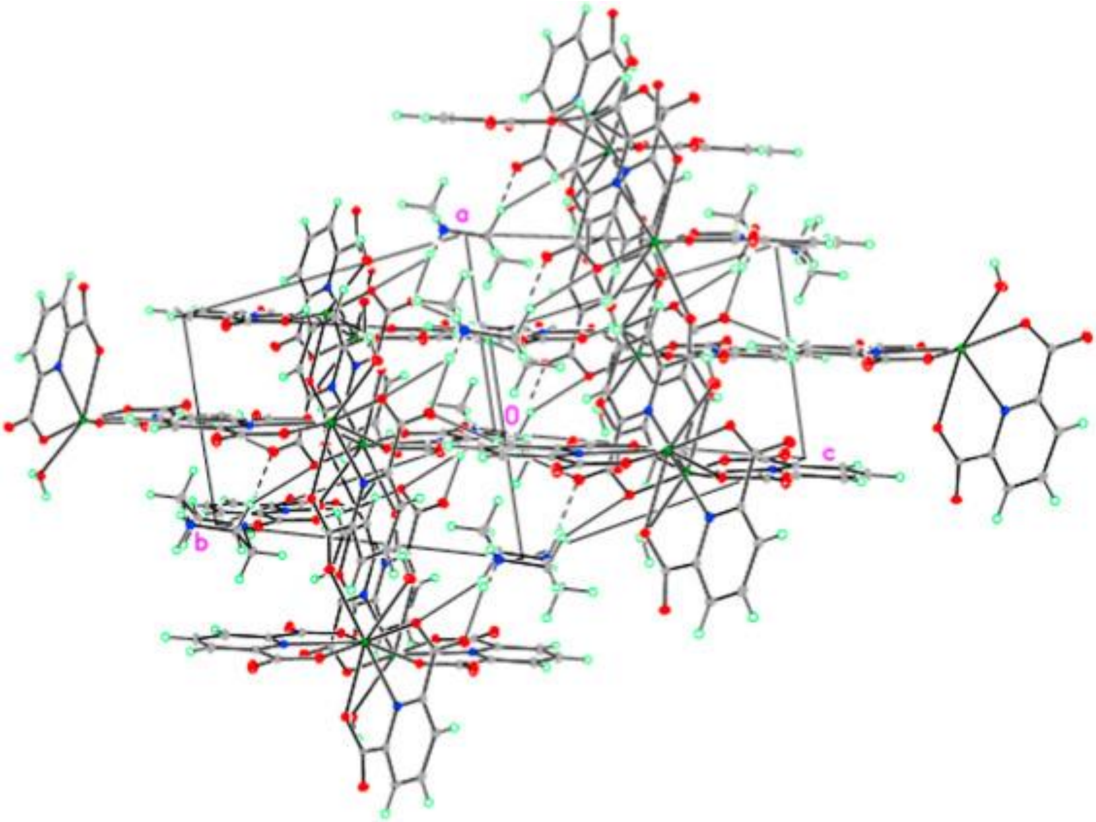

(b)

Figure 20. (a) Asymmetric unit of **32** **(b)** 3-D network of **32**.

The IR spectrum of the compound exhibits the bands at 3426 cm^{-1} for ν(N-H) vibrations of complementary ion H_2Ppz^{2+} and at 3247 cm^{-1} for ν(O-H) vibrations of coordinate H_2O [106]. Free ligand and the Sm(III) complex showed ν(C=O) stretching vibrations at 1688 cm^{-1} and 1622 cm^{-1}, respectively. This shift indicates that the oxygen atom of the carbonyl group is coordinated to the Sm(III) ion. The bands observed at 764 cm^{-1} for the ν(Sm-O) vibration and at 433 cm^{-1} for the ν(Sm-N) vibration indicate that the O- and N-atoms of the Py-2,6-Dc^{2-} ligand are coordinated to the Sm(III) ion [107, 108].

2.3.3.2.5. Mixed-ligand complex $(H_2Ppz)_3[Tb_2(Py\text{-}2,6\text{-}Dc)_6]\cdot 15H_2O$ (33)

Hydrothermally synthesized Tb(III) complex [109], $(H_2Ppz)_3[Tb_2(Py\text{-}2,6\text{-}Dc)_6]\cdot 15H_2O$ (**33**), has an interesting structure because it contains 1-D water chains consisting of $(H_2O)_{20}$ clusters. The complex is expanded into a 3-D supramolecular network structure *via* H-bonds by π–π stacking interactions. Besides the Tb(III) ion, the asymmetric unit of the complex consists of a Py-2,6-Dc^{2-} ion as ligand, one half of the H_2Ppz^{2+} cation as a counter ion, and five lattice water molecules (Figure 21a). The Tb(III) center is coordinated with three N and six O atoms from the three Py-2,6-Dc^{2-} ligands and has a slightly distorted tricapped trigonal prismatic geometry (Figure 21b).

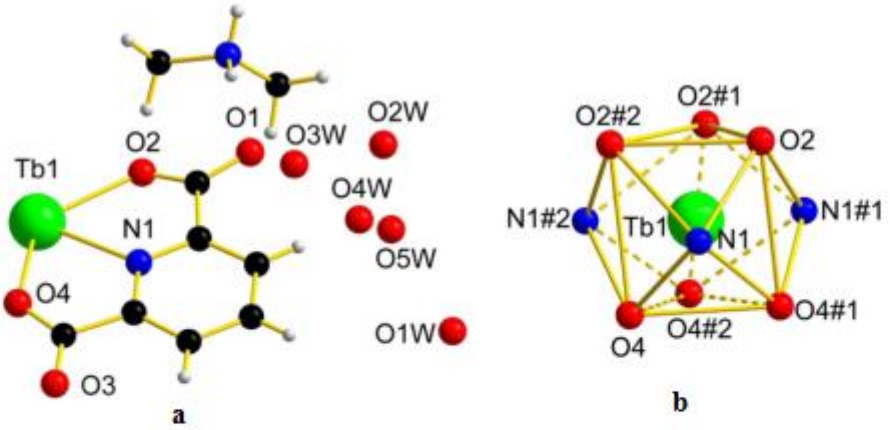

Figure 21. (a) Binding pattern of Tb1 in complex **33** (b) Distorted tricapped trigonal prism image of Tb1 in complex **33.**

2.3.3.2.6. Mixed-ligand complex $(H_2Ppz)[Ce_2(Py\text{-}2,6\text{-}Dc)_4(H_2O)_4]\cdot H_2O$ (34)

The binuclear unit of $(H_2Ppz)[Ce_2(Py\text{-}2,6\text{-}Dc)_4(H_2O)_4]\cdot H_2O$ (**34**) consists of Ce(III) cations bridged with two dipic anions [110] (Figure 22). In complex, Ce^{3+} ion is nine coordinated. The H-bonds in the molecular structure of the complex connect the binuclear units, piperazine and water molecules in a 3-D architecture.

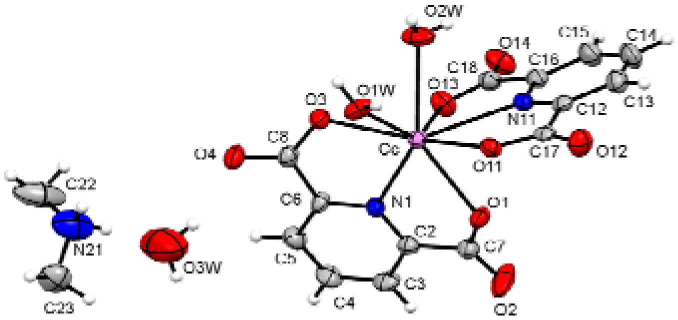

Figure 22. The asymmetric unit of $(H_2Ppz)[Ce_2(Py\text{-}2,6\text{-}Dc)_4(H_2O)_4]\cdot(H_2O)$ (**34**).

2.3.3.2.7. Mixed-ligand complexes $(H_2Ppz)_n[La_2(Py\text{-}2,6\text{-}Dc)4(H_2O)_2]_n$ (35) and $(H_2Ppz)_n[Nd_2(Py\text{-}2,6\text{-}Dc)_4(H_2O)_2]_n$ (36)

Two Ln-MOFs obtained by the hydrothermal method, $(H_2Ppz)_n[La_2(Py\text{-}2,6\text{-}Dc)4(H_2O)_2]_n$ (**35**) and $(H_2Ppz)_n[Nd_2(Py\text{-}2,6\text{-}Dc)_4(H_2O)_2]_n$ (**36**) contains the $Py\text{-}2,6\text{-}Dc^{2-}$ anion and water molecules as ligands and exists as a complementary ion [111]. The asymmetric unit of complexes contain one Ln(III) ion, two $Py\text{-}2,6\text{-}Dc^{2-}$ fragments, an aqua ligand and half of the uncoordinated piperazine ring. Geometry of complexes is distorted mono-capped square antiprism with four oxygen atoms on one face (O(1), O(2), O(5) and O(7)) and four nitrogen atoms on the opposite face (N(2), O(3), O(5) and O(9)) (Figure 23).

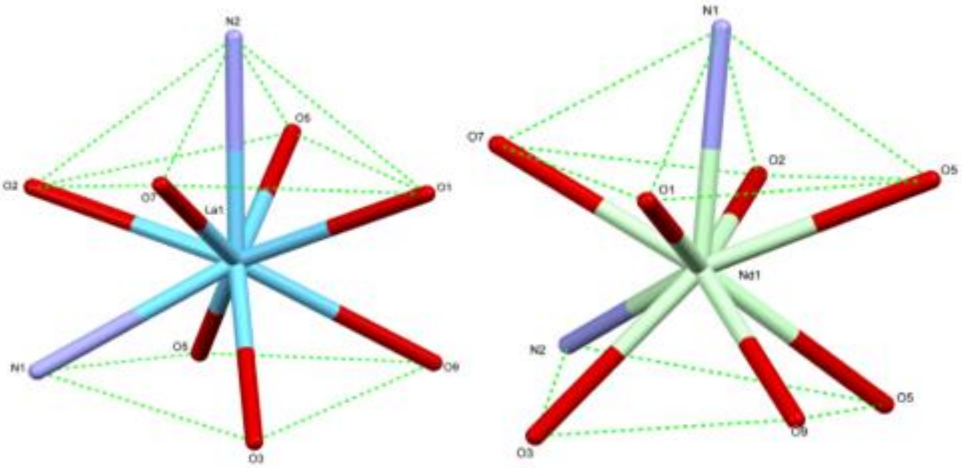

Figure 23. (a) Mono-capped square antiprism coordination geometry of La(III) (**35**) and (b) Nd(III) (**36**) ions.

3. CONCLUSIONS

In this short review, proton transfer salts and their complexes and mixed-ligand complexes obtained from pyridine-dicarboxylic acids and piperazines between 2009 and 2021 were investigated. Between these years, proton transfer salts and metal complexes obtained from the reaction of pyridine-2,4-, 3,4- and 3,5-dicarboxylic acids with piperazines were not encountered. In the examination, it was seen that Py-2,6-H_2Dc was used the most, followed by Py-2,5-H_2Dc. It was observed that piperazine was used mostly, as a base in the reactions, but its derivatives were used very little. Here in, metal ions of proton transfer salts and mixed ligand metal complexes include s-, p-, and mostly d- and f-block metals. It has been determined that H-bonding has an important contribution to the stabilization of the 3-D networks formed in the molecular structures of the compounds studied.

ACKNOWLEDGEMENT

I would like to thank Dr Halil İlkimen for his help in the literature survey.

REFERENCES

[1] Gomtsyan, A., (2012), Heterocycles in drugs and drug discovery, Chemistry of Heterocyclic Compounds, 48(1), 7–10.

[2] Chandrika, N. T., Shrestha, S. K., Ngo, H. X., Tsodikov, O. V., Howard, K. C., Garneau-Tsodikova, S., (2017), Alkylated Piperazines and Piperazine-Azole Hybrids as Antifungal Agents, Journal of Medicinal Chemistry, 61(1), 158–173.

[3] Pytka, K., Rapacz, A., Zygmunt, M., Olczyk, A., Waszkielewicz, A., Sapa, J., Filipek, B., (2015), Antidepressant-like activity of a new piperazine derivative of xanthone in the forced swim test in mice: The involvement of serotonergic system, Pharmacology Reports, 67(1), 160–165.

[4] Parai, M. K, Panda, G., Srivastava, K., Puri, S. K, (2008), Design, synthesis and antimalarial activity of benzene and isoquinoline sulfonamide derivatives, Bioorganic and Medicinal Chemistry Letters, 18(2), 776–781.

[5] Brown, A. M, Patch, T.L., Kaumann, A. J., (1991), The antimigraine drugs ergotamine and dihydroergotamine are potent 5-HT1C receptor agonists in piglet choroid plexus, British Journal of Pharmacology, 104, 45–48.

[6] Le Bihan, G., Rondu, F., Pele-Tounian A, Wang, X., Lidy S, Touboul, E., Lamouri, A., Dive, G., Huet, J., Pfeiffer, B., Renard, P., Guardiola-Lemaitre, B., Manechez, D., Penicaud, L., Ktorza, A., Godfroid, J. J., (1999), Design and Synthesis of Imidazoline Derivatives Active on Glucose Homeostasis in a Rat Model of Type II Diabetes. 2, Journal of Medicinal Chemistry, 42(9), 1587–1603.

[7] Ranise, A., Spallarossa, A., Bruno, O., Schenone, S., Fossa, P., Menozzi, G., Bondavalli, F., Mosti, L., Capuano, A., Mazzeo, F., Falcone, G., Filippelli, W., (2003), Synthesis of N-substituted-N-acylthioureas of 4-substituted piperazines endowed with local anaesthetic, antihyperlipidemic, antiproliferative activities and antiarrythmic, analgesic, antiaggregating actions, Farmaco, 58(9), 765–780.

[8] McNair, T. J., Wibin, F. A, Hoppe, E. T, Schmidt, J. L., dePeyster, F. A., (1963), Antitumor action of several new piperazine derivatives compared to certain standard anticancer agents, Journal of Surgical Research, 3(3), 130–136.

[9] Kumar, C. S. A, Swamy, S. N, Thimmegowda, N. R, Prasad, S. B. B, Yip, G. W, Rangappa, K. S., (2007), Synthesis and evaluation of 1-benzhydryl-sulfonyl-piperazine derivatives as inhibitors of MDA-MB-231 human breast cancer cell proliferation, Medicinal Chemistry Research, 16(4), 179–187.

[10] Ahmadi, A., Khalili, M., Nafarie, A., Yazdani, A. Nahri-Niknafs, B., (2012), Synthesis and anti-inflammatory effects of new piperazine and ethanolamine derivatives of H1-antihistaminic drugs, Mini-Reviews in Medicinal Chemistry, 12(12), 1282–1292.

[11] Guo, J., Tao, H., Alasadi, A., Huang, Q., Jin, S., (2019), Niclosamide piperazine prevents high-fat diet-induced obesity and diabetic symptoms in mice. Eating and Weight Disorders - Studies on Anorexia, Bulimia and Obesity, Eating and Weight Disorders, 24, 91–96.

[12] Waszkielewicz, A. M., Kubacka, M., Panczyk, K., Mogilski, S., Siwek, A., Glich-Lutwin, M., Grybos, A., Filipek, B., (2016), Synthesis and activity of newly designed aroxyalkyl or aroxyethoxyethyl derivatives of piperazine on the cardiovascular and the central nervous systems, Bioorganic Medicinal Chemistry Letters, 26, 5315–5321.

[13] Sharif, M. A, Aghabozorg, H., Shokrollahi, A., Kickelbick, G., Moghimi, A., Shamsipur, M., (2006), Novel Proton Transfer Compounds Containing 2,6-Pyridinedicarboxylic Acid and Melamine and Their PbII Complex: Synthesis, Characterization, Crystal Structure and Solution Studies, Polish Journal of Chemistry, 80 847- 863.

[14] Moghimi, A., Sharif, M. A., Shokrollahi, A., Shamsipur, M., Aghabozorg, H., (2005), A Novel Proton Transfer Compound Containing 2, 6-Pyridinedicarboxylic Acid and Creatinine and its Zinc(II) Complex ? Synthesis, Characterization, Crystal Structure, and Solution Studies, Zeitschrift für anorganische und allgemeine Chemie, 631(5), 902–908.

[15] Aghabozorg, H., Ramezanipour, F., Nakhjavan, B., Soleimannejad, J., Attar Gharamaleki, J., Sharif, M. A., (2007), Different complexation behavior of a proton transfer compound obtained from 1,10-phenanthroline and pyridine-2,6-dicarboxylic acid with Sn(IV), Sb(III) and Tl(I), Crystal Research and Technology, 42(11), 1137–1144.

[16] Zhang, M., Chen, C., Wang, Q., Fu, W., Huang, K., Zhou, W., (2017), Metal-Organic Framework with Functionalized Piperazine Exhibiting Enhanced CH_4 Storage, Journal of Materials Chemistry A, 5, 349–354.

[17] Lehn, J. -M., (1988), Supramolecular Chemistry—Scope and Perspectives Molecules, Supermolecules, and Molecular Devices (Nobel Lecture), Angewandte Chemie International Edition, 27(1), 89–112.

[18] Csöregh, I., Weber, E., Hens, T., (1998), The Role of Chloro Substituents in Solid Inclusion Formation. Crystal Structures Formed by a Bulky Hydroxy Host with Ethyl Acetate (2:1) and Cyclohexylamine (1:2) as Guest, Supramolecular Chemistry, 10(1), 133–142.

[19] Groeneman, R. H., MacGillivray, L. R., Atwood, J. L., (1999), One-Dimensional Coordination Polymers Based upon Bridging Terephthalate Ions, Inorganic Chemistry, 38(2), 208–209.

[20] Khalil, M. M., Attia, A. E., (1999), Potentiometric Studies on the Binary and Ternary Complexes of Copper(II) Containing Dipicolinic Acid and Amino Acids, Journal of Chemical and Engineering Data, 44(2), 180–184.

[21] Tochikubo, K., Hachisuka, Y., Murachi, T., (1968), Properties of Glucose Dehydrogenase from Vegetative Cells ofBacillus subtilisand Effect of Dipicolinic Acid and its Chemical Analogues on the Enzyme, Japanase Journal of Microbiology, 12(4), 435–440.

[22] Martin, B. L., (1997), Selective Activation of Calcineurin by Dipicolinic Acid, Archives Biochemistry and Biophysics, 345(2), 332–338.

[23] Bannister, W. H., Bannister, J. V., Searle, A. J. F., Thornalley, P. J., (1983), The reaction of superoxide radicals with metal picolinate complexes, Inorganica Chimica Acta, 78, 139–142.

[24] Aghabozorg, H., Manteghi, F., Sheshmani, S., (2008), A brief review on structural concepts of novel supramolecular proton transfer compounds and their metal complexes, Journal of Iranian Chemical Society, 5(2), 184–227.

[25] Moghimi, A., Moosavi, S. M., Kordestani, D., Maddah, B., Shamsipur, M., Aghabozorg, H., Kickelbick, G., (2007), Pyridine-2,6-bis(monothiocarboxylic) acid and 2-aminopyridine as building blocks of a novel proton transfer compound: Solution and X-ray crystal structural studies, Journal of Molecular Structure, 828(1-3), 38–45.

[26] Tunca, E., Bülbül, M., İlkimen, H., Canlıdinç, R. S., Yenikaya, C., (2020), Investigation of the effects of the proton transfer salts of 2-aminopyridine derivatives with 5-sulfosalicylic acid and their Cu(II) complexes on cancer-related carbonic anhydrases: CA IX and CA XII, Chemical Papers, 74, 2365–2374.

[27] İlkimen, H., Yenikaya, C., Sarı, M., Bülbül, M., Tunca, E., Dal, H. (2013), Synthesis and characterization of a proton transfer salt between 2,6-pyridinedicarboxylic acid and 2-aminobenzothiazole, and its complexes and their inhibition studies on carbonic anhydrase isoenzymes, Journal of Enzyme Inhibition and Medicinal Chemistry, 29(3), 353–361.

[28] İlkimen, H., Yenikaya, C., Sarı, M., Bülbül, M., Tunca, E., Süzen, Y. (2013), Synthesis and characterization of a proton transfer salt between dipicolinic acid and 2-amino-6-methylbenzothiazole and its complexes, and their inhibition studies on carbonic anhydrase isoenzymes, Polyhedron, 61, 56–64.

[29] Yang, G., Park, S.-J., (2019), Conventional and Microwave Hydrothermal Synthesis and Application of Functional Materials: A Review, Materials, 12(7), 1177–1194.

[30] Li, G., Li, L., Feng, S., Wang, M., Zhang, L., Yao, X., (1999), An Effective Synthetic Route for a Novel Electrolyte: Nanocrystalline Solid Solutions of (CeO_2)1-x(BiO1.5)x, Advanced Materials, 11(2), 146–149.

[31] Cheetham, A. K., Férey, G., Loiseau, T., (1999), Open-Framework Inorganic Materials, Angewandte Chemie International Edition, 38(22), 3268–3292

[32] Feng, S., Greenblatt, M., (1992), Galvanic cell type humidity sensor with NASICON-based material operative at high temperature, Chemical Materials, 4(6), 1257–1262.

[33] Feng, S., Xu, R., (2001), New Materials in Hydrothermal Synthesis, Accounts of Chemical Research, 34(3), 239–247.

[34] Che, G.-B., Liu, S.-Y., Zhang, Q., Liu, C.-B., Zhang, X.-J., (2015), Syntheses, structures and photoluminescence of lanthanide-organic frameworks assembled from multifunctional N,O-donor ligand, Journal of Solid State Chemistry, 225, 378–382.

[35] Sun, F., Yin, Z., Sun, C. -G., Kurmoo, M., Zeng, M. -H., (2014), Design, structure and luminescent properties of a novel two-dimensional Cd(II) coordination polymer constructed from in situ generated 1-methyl-2-(3H-[1–3]triazol-4-yl)-1H-benzoimidazole, Inorganic Chemistry Communications, 43, 78–80.

[36] You, L. -X., Li, Z. -G., Ding, F., Wang, S .-J., Ren, B. -Y., Sun, Y. -G., (2014), Synthesis, structure and luminescence properties of lanthanide coordination polymers using in situ decarboxylation of a H_3cppdc ligand, Inorganic Chemistry Communications, 46, 340–343.

[37] Semerci, F., Yeşilel, O. Z., Ölmez, H., Büyükgüngör, O., (2014), Supramolecular assemblies of copper(II)–pyridine-2,3-dicarboxylate complexes with N-donor ligands and clustered water molecules, Inorganica Chimica Acta, 409, 407–417.

[38] Han, Z., Li, J., Gao, J., (2006), Synthesis, crystal structure and magnetic properties of 2D bi-layered coordination polymer, Journal of Coordination Chemistry, 59(14), 1641–1647.

[39] Wibowo, A. C., Smith, M. D., zur Loye, H. -C., (2011), A new Kagomé lattice coordination polymer based on bismuth and pyridine-2,5-dicarboxylate: structure and photoluminescent properties, Chemical Communications, 47(26), 7371–7373.

[40] Hamdy, L. B., Raithby, P. R., Thomas, L. H., Wilson, C. C., (2014), Self-assembly synthesis of precursors to potential open framework alkali earth metal–organic complexes, New Journal of Chemistry, 38(5), 2135–2143.

[41] Shi, Q., Zhang, S., Wang, Q., Ma, H., Yang, G., Sun, W. -H., (2007), Synthesis and crystal structure of metal-organic frameworks $[Ln_2(pydc\text{-}3,5)_3(H_2O)_9]n3nH_2O$ (Ln=Sm, Eu, Gd, Dy; pydc-3,5=pyridine-3,5-dicarboxylate) along with the photoluminescent property of its europium one, Journal of Molecular Structure, 837(1-3), 185–189.

[42] Song, Y., Wang, X., Zhang, S., Wang, J., Gao, S., Chen, S., (2016), Lanthanide-Coordination Polymers with Pyridinedicarboxylic Acids: Syntheses, Structures, and Luminescent Properties, Zeitschrift für anorganische und allgemeine Chemie, 642(11-12), 681–691.

[43] Nandi, G., Thakuria, R., Titi, H. M., Patra, R., Goldberg, I., (2014), Synthesis, structure, topology and magnetic properties of new coordination polymers based on 5(-Br/-COOH)-substituted nicotinic acid, CrystEngComm, 16, 5244–5256.

[44] Chauhan, S., Patel, P., Pandya, V., (2014), Studies of Some Novel Chromium Pyridine Dicarboxylate Complexes, Oriental Journal of Chemistry, 30(4), 1763–1769.

[45] Barszcz, B., Hodorowicz, M., Jablonska-Wawrzycka, A., Masternak, J., Nitek, W. Stadnicka, K., (2010), Comparative study on Cd(II) and Ca(II) model complexes with pyridine-2,3-dicarboxylic acid: Synthesis, crystal structure and spectroscopic investigation, Polyhedron, 29, 1191–1200.

[46] Li, L.-J., Li, Y., (2004), Hydrothermal synthesis and crystal structure of a novel 2-D coordination polymer $[Mn_2(pdc)_2(H_2O)_3]n2nH_2O$ (pdc=pyridine-2,3-dicarboxylate), Journal of Molecular Structure, 694(1-3), 199–203.

[47] Kowalik, M., Masternak, J., Łakomska, I., Kazimierczuk, K., Zawilak-Pawlik, A., Szczepanowski, P., Barszcz, B., (2020), Structural Insights into New Bi(III) Coordination Polymers with Pyridine-2,3-Dicarboxylic Acid: Photoluminescence Properties and Anti-Helicobacter pylori Activity, International Journal of Molecular Sciences, 21(22), 8696–8721.

[48] Aghabozorg, H., Manteghi, F., Ghadermazi, M., (2008), Piperazinediium bis(2-carboxypyridine-3-carboxylate), Acta Crystallographica, E64(1), o230–o230.

[49] Aghabozorg, H., Daneshvar, S., Motyeian, E., Manteghi, F., Khadivi, R., Ghadermazi, M., Shamsipur, M., (2009), Synthesis and crystal structure of Mn(II) and Hg(II) compounds and solution studies of Mn(II), Zn(II), Cd(II) and Hg(II) compounds based on piperazinediium pyridine-2,3-dicarboxylate, Journal of Iranian Chemical Society, 6(3), 620–637.

[50] Aghabozorg, H., Daneshvar, S., Motyeian, E., Ghadermazi, M., Gharamaleki, A. J., (2007), catena-Poly[piperazindiium [zincate(II)-bis(μ-pyridine-2,3-dicarboxylato)-$\kappa^3N,O^2:O^3;\kappa^3O^3:N,O^2$] tetrahydrate], Acta Crystallographica, E63, m2468-m2469.

[51] Aghabozorg, H., Motyeian, E., Khadivi, R., Ghadermazi, M., Manteghi, F., (2008), catena-Poly[[triaquacadmium(II)]-μ-pyridine-2,3-dicarboxylato-$\kappa^3N,O^2:O^3$], Acta Crystallographica, E64, m320-m321.

[52] Manteghi, F., Ghadermazi, M., Kakaei, N., (2011), Piperazine-1,4-diium pyridine-2,3-dicarboxylate methanol monosolvate, Acta Crystallographica, E67(5), o1122–o1122.

[53] Zhang, X., Huang, D., Chen, C., Liu, Q., Liao, D., Li, L., (2005), Synthesis, structural characterization and magnetic property of metal 2,5-pyridine dicarboxylate complex, Inorganic Chemistry Communications, 8(1), 22–26.

[54] Xie, C., Zhang, B., Wang, X., Wang, R., Shen, G., Shen, D., (2006), The synthesis and structure of a novel alternating 1-D cobalt coordination polymer $[Co(2,5\text{-}PDC)_2(H_2O)_2Co(H_2O)_4]\cdot 4H_2O$, Journal of Chemical Crystallography, 37(1), 25–29.

[55] Plater, M. J., St. J. Foreman, M. R., Howie, R. A., Lachowski, E. E., (1998), Hydrothermal Synthesis and Characterisation of $M(pdc)\cdot 3H_2O$ (pdc=2,5-pyridinedicarboxylate); M=Co, Ni, CoxNiy (x=0.4–0.6, y=0.6–0.4), Journal of Chemical Research, Part S (12), 754–755.

[56] Lee, J., Shim, H., Park, Y., Park, S., Shin, J., Yang, W., Lee, S., (2002), 2,5-Pyridinedicarboxylic acid derivatives as non-Nucleosidic Reverse transcriptase inhibitors of Hepatitis B Virus, Bioorganic and Medicinal Chemistry Letters, 12(19), 2715–2717.

[57] Tucker, H., Thomas, D. F., (1992), Novel inhibitors of prolyl 4-hydroxylase. 2. 5-Amide substituted pyridine-2-carboxylic acids, Journal of Medicinal Chemistry, 35(5), 804–807.

[58] Sengupta, P., Ghosh, S., Mak, T. C., (2001), A new route for the synthesis of bis(pyridine dicarboxylato)bis(triphenylphosphine) complexes of ruthenium(II) and X-ray structural characterisation of the biologically active trans-$[Ru(PPh_3)_2(L_1H)_2]$ (L_1H_2=pyridine 2,3-dicarboxylic acid), Polyhedron, 20(9-10), 975–980.

[59] Patrick, B. O., Stevens, C. L., Storr, A., Thompson, R. C, (2005), Coordination polymers incorporating copper(II) and manganese(II) centers bridged by pyridinedicarboxylate ligands: Structure and magnetism, Polyhedron, 24(16-17), 2242–2249.

[60] Süss-Fink, G., Cuervo, L. G., Therrien, B., Stoeckli-Evans, H., Shul'pin, G. B., (2004), Mono and oligonuclear vanadium complexes as catalysts for alkane oxidation: synthesis, molecular structure, and catalytic potential, Inorganica Chimica Acta, 357(2), 475–484.

[61] Sun, L.-P., Niu, S.-Y., Jin, J., Yang, G.-D., Ye, L., (2006), Synthesis, Structure and Surface Photovoltage of a Series of NiII Coordination Polymers, European Journal of Inorganic Chemistry, 2006(24), 5130–5137.

[62] Kita, E., Marai, H., Zając, K., (2007), Synthesis and kinetic studies in aqueous solution on chromium(III) complexes with isocinchomeronic acid—potential new biochromium sources, Transitition Metal Chemistry, 33(2), 211–217.

[63] Jin, J., Li, D., Li, L., Han, X., Cong, S., Chi, Y., Niu, S., (2011), Synthesis, crystal structure and surface photo-electric property of a series of Co(II) coordination polymers and supramolecules, Inorganica Chimica Acta, 379(1), 44–55

[64] Jin, J., Ding, Y., Gong, Y.-Y., Cong, S.-M., Chi, Y.-X., Zhang, G.-N., Niu, S.-Y., (2013), Synthesis, structure and surface photo-electric property of Ni(II) complexes, Inorganica Chimica Acta, 399, 227–235.

[65] Manna, S. C., Jana, A. D., Drew, M. G. B., Mostafa, G., Ray Chaudhuri, N., (2008), Polymorphism in $[Co(SCN)_4(ppz\text{-}H)_2]$ (ppz, piperazine), Polyhedron, 27(4), 1280–1286.

[66] Ay, B., Yildiz, E., Kani, İ., (2016), Novel heteroleptic lanthanide organic frameworks containing pyridine-2,5-dicarboxylic acid and in situ generated piperazine-2,5-dicarboxylic acid from piperazine: Hydrothermal synthesis and luminescent properties, Journal of Solid State Chemistry, 233 (2016) 44–51.

[67] Zhang, L., Guo, J., Meng, Q., Pang, H., Chen, Z., Sun, D., (2012), Two novel isostructural Ln (III) 3D frameworks supported by 3,6-dibromobenzene-1,2,4,5-tetracarboxylic acid and in situ generated oxalate: Syntheses, characterization and photoluminescent property, Inorganic Chemistry Communications, 26, 51–55.

[68] Hu, J. -Y., Wen, J., Yang, X . -G., Chen, M., Liu, C.-S., (2013), A 3-D lanthanide–organic framework based on in situ formed benzene-1,2,3,4-tetracarboxylate ligand, Inorganic Chemistry Communications, 33, 25–28.

[69] Singha, D. K., Majee, P., Mondal, S. K., Mahata, P., (2017), Selective Luminescence-Based Detection of Cd^{2+} and Zn^{2+} Ions in Water Using a Proton-Transferred Coordination Polymer-Amine Conjugate Pair, Chemistry Select, 2(11), 3388–3395.

[70] Singha, D. K., Mahata, P., (2017), Coordination polymer-derived nano-sized zinc ferrite with excellent performance in nitro-explosive detection, Dalton Transactions, 46(34), 11344–11354.

[71] Debamalya, G., Debal, K. S., Lebedev, O. I., Seikh, M. M., Mahata, P., (2019), A remarkable annealing time effect on the magnetic properties of single-source coordination polymer precursor-derived $CoFe_2O_4$ nanoparticles, New Journal of Chemistry, 43(48), 19044–19052.

[72] Debamalya, G., Ananya, P., Susanta, G., Arup, G., Seikh, M. M., Mahata P., (2019), Metal Ion Sensing and Electrochemical Behaviour of MOF Derived ZnCo2O4, European Journal of Inorganic Chemistry, 3076–3083.

[73] Moghimi, A., Sharif, M. A., Shokrollahi, A., Shamsipur, M., Aghabozorg, H., (2005), A Novel Proton Transfer Compound Containing 2, 6-Pyridinedicarboxylic Acid and Creatinine and its Zinc(II) Complex-Synthesis, Characterization, Crystal Structure, and Solution Studies, Zeitschrift für anorganische und allgemeine Chemie, 631(5), 902–908.

[74] Aghabozorg, H., Akbari Saei, A., Ramezanipour, F., (2005), 2,6-Diaminopyridinium pyridinium-2,6-dicarboxylate: a redetermination, Acta Crystallographica, E61(10), o3242–o3244.

[75] Aghabozorg, H., Manteghi, F., Ghadermazi, M., (2007), Ammonium 6-carboxypyridine-2-carboxylate, Acta Crystallographica, E63(11), o4454–o4454.

[76] Sheshmani, S., Aghabozorg, H., Ghadermazi, M (2007), Piperazinediium pyridine-2,5-dicarboxylate dehydrate, Acta Crystallographica, E63(6), o2869–o2869.

[77] Aghabozorg, H., Ghadermazi, M., Sheshmani, S., (2006), A novel proton-transfer compound: piperazinium oxalate monohydrate, Acta Crystallographica, E62(8), o3287–o3289.

[78] Gonzalez-Baró, A. C., Castellano, E. E., Piro, O. E., Parajón-Costa, B. S., (2005), Synthesis, crystal structure and spectroscopic characterization of a novel bis (oxo-bridged) dinuclear vanadium(V)–dipicolinic acid complex, Polyhedron, 24(1), 49–55.

[79] Setlow B, Setlow P., (1993), Dipicolinic acid greatly enhances the production of spore photoproduct in bacterial spores upon ultraviolet irradiation, Applied and Environmental, Microbiology, 59, 640–43.

[80] Olar, R., Badea, M., Marinescu, D., Chifiriuc, C.-M., Bleotu, C., Grecu, M. N., Finaru, A., (2010), Prospects for new antimicrobials based on N,N-dimethylbiguanide complexes as effective agents on both planktonic and adhered microbial strains, European Journal of Medicinal Chemistry, 45(7), 2868–2875.

[81] Gao, H.-L., Yi, L., Zhao, B., Zhao, X.-Q., Cheng, P., Liao, D.-Z., Yan, S.-P., (2006), Synthesis and Characterization of Metal−Organic Frameworks Based on 4-Hydroxypyridine-2,6-dicarboxylic Acid and Pyridine-2,6-dicarboxylic Acid Ligands, Inorganic Chemistry, 45(15), 5980–5988.

[82] Zhao, B., Yi, L., Dai, Y., Chen, X.-Y., Cheng, P., Liao, D.-Z., Jiang, Z.-H., (2005), Systematic Investigation of the Hydrothermal Syntheses of Pr(III)−PDA (PDA=Pyridine-2,6-dicarboxylate Anion) Metal−Organic Frameworks, Inorganic Chemistry, 44(4), 911–920.

[83] Aghabozorg, H., Ghadermazi, M., Manteghi, F., Nakhjavan, B., (2006), A Proton Transfer Compound of Piperazine with Pyridine-2,6-dicarboxylic Acid and Its Palladium(II) and Thallium(III) Complexes – Synthesis, Characterization and Crystal Structure, Zeitschrift für anorganische und allgemeine Chemie, 632(12-13), 2058–2064.

[84] Aghabozorg, H., Manteghi, F., Ghadermazi, M., Mirzaei, M., Salimi, A. R., Shokrollahi, A., Eshtiagh-Hosseini, H., (2009), A novel supramolecular compound of cadmium(II): Synthesis, characterization, crystal structure, ab initio HF, DFT calculations and solution study, Journal of Molecular Structure, 919(1-3), 381–388.

[85] Aghabozorg, H., Ghadermazi, M., Zabihi, F., Nakhjavan, B., Soleimannejad, J., Sadr-khanlou, E., Moghimi, A., (2008), Novel Complexes of Zinc(II) with Different Proton Transfer Ion Pairs Obtained from Dipicolinic Acid: Synthesis, Characterization and X-ray Crystal Structure, Journal of Chemical Crystallography, 38(9), 645–654.

[86] Aghabozorg, H., Ghasemikhah, P., Ghadermazi, M., Attar Gharamaleki, J., Sheshmani, S., (2006), Piperazinium bis(pyridine-2,6-dicarboxylato)mercurate(II) hexahydrate, Acta Crystallographica, E62(9), m2269–m2271.

[87] Aghabozorg, H., Manteghi, F., Ghadermazi, M., Mirzaei, M., Salimi, A. R., Eshtiagh-Hosseini, H., (2010), Synthesis, X-Ray characterization and molecular structure of a novel supramolecular compound of antimony(III); Theoretical investigation on molecular and electronic properties based on the ab initio HF and various DFT methods, Journal of Iranian Chemical Society, 7(2), 500–509.

[88] Aghabozorg, H., Nemati, A., Derikvand, Z., Ghadermazi, M., (2008), Poly[piperazinediium [[aquabismuthate(III)]-di-µ-pyridine-2,6-dicarboxylato-bismuthate(III)-di-µ-pyridine-2,6-dicarboxylato] monohydrate], Acta Crystallographica, e64(2), m374–m374.

[89] Aghabozorg, H., Motieiyan, E., Salimi, A. R., Mirzaei, M., Manteghi, F., Shokrollahi, A., Eshtiagh-Hosseini, H., (2010), Piperazinediium, Zr(IV) and Ce(IV) pyridine-2,6-dicarboxylates: Syntheses, characterizations, crystal structures, ab initio HF, DFT calculations and solution studies, Polyhedron, 29(5), 1453–1464.

[90] Aghabozorg, H., Moghimi, A., Manteghi, F., Ranjbar, M., (2005), A Nine-Coordinated Zr(IV) Complex and a Self-Assembling System Obtained from a Proton Transfer Compound Containing 2,6-Pyridinedicarboxylate and 2,6-Pyridinediammonium; Synthesis and X-ray Crystal Structure, Zeitschrift für anorganische und allgemeine Chemie, 631(5), 909–913.

[91] Ghadermazi, M., Sheshmani, S., Shokrollahi, A., Arokhloo, J. K., (2014), Metal–organic polymers of Sr(II) and Ce(IV): structural studies, supramolecular synthons, and potentiometric measurements, Journal of Coordination Chemistry, 67(21), 3492–3509.

[92] Chandramohan, A., Bharathikannan, R., Kandhaswamy, M. A., Chandrasekaran, J., Kandavelu, V., (2008), Synthesis, crystal growth, spectral, thermal and optical properties of acenaphthene picrate, Crystal Research and Technology, 43(1), 93–98.

[93] K. Nakamoto, Infrared and Raman Spectra of Inorganic and Coordination Compounds, Part B, 5th Edn, Wiley, New York (1997)

[94] Jayaraman, K., Choudhury, A., Rao, C. N. R., (2002), Sulfates of organic diamines: hydrogen-bonded structures and properties, Solid State Sciences, 4(3), 413–422.

[95] Singh, M., Lofland, S. E., Ramanujachary, K. V., Ramanan, A., (2010), Crystallization of Anderson−Evans Type Chromium Molybdate Solids Incorporated with a Metal Pyrazine Complex or Coordination Polymer, Crystal Growth and Design, 10(12), 5105–5112.

[96] Pavani, K., Singh, M., Ramanan, A., (2011), Oxalate Bridged Copper Pyrazole Complex Templated Anderson-Evans Cluster Based Solids, Australian Journal of Chemistry, 64(1), 68–76.

[97] Büyükkıdan, N., Yenikaya, C., İlkimen, H., Karahan, C., Darcan, C., Şahin, E., (2012), Synthesis, characterization, and antimicrobial activity of a novel proton salt and its Cu(II) complex, Russian Journal of Coordination Chemistry, 39(1), 96–103.

[98] Büyükkıdan, N., Yenikaya, C., İlkimen, H., Karahan, C., Darcan, C., Korkmaz, T., Süzen, Y., (2015), Synthesis, characterization and biological activities of metal(II) dipicolinate complexes derived from pyridine-2,6-dicarboxylic acid and 2-(piperazin-1-yl)ethanol, Journal of Molecular Structure, 1101, 139–146.

[99] Kirillova, M. V., Guedes da Silva, M. F. C., Kirillov, A. M., Fraústo da Silva, J. J. R., Pombeiro, A. J. L., (2007), 3D hydrogen bonded heteronuclear CoII, NiII, CuII and ZnII aqua complexes derived from dipicolinic acid, Inorganica Chimica Acta, 360(2), 506–512.

[100] Yeşilel, O. Z., İlker, İ., Refat, M. S., Ishida, H., (2010), Syntheses and characterization of two copper pyridine-dicarboxylate compounds containing water clusters, Polyhedron, 29(11), 2345–2351.

[101] Raissi Shabari, A., Ghoddoosi, N., Pourayoubi, M., Moradi, S., (2011), Piperazine-1,4-diium bis(pyridine-2,6-dicarboxylato-κ3O2,N,O6)cobaltate(II) tetrahydrate, Acta Crystallographica, E67(7), m985–m986.

[102] Thirumurugan, A., Cheetham, A. K., (2010), Anionic Metal-Organic Frameworks of Bismuth Benzenedicarboxylates: Synthesis, Structure and Ligand-Sensitized Photoluminescence, European Journal of Inorganic Chemistry, 3823–3828.

[103] Hakimi, M.,Motieiyan, E., Bertolotti, F., Marabello, D., , Nunes Rodrigues, V. H., (2015),Three new bismuth(III) pyridine-2,6-dicarboxylate compounds: Synthesis, characterization and crystal structures, Journal of Molecular Structure, 1099, 523–533.

[104] Ay, B., Karaca, S., Yildiz, E., Lopez, V., Nanao, M. H., Zubieta, J., (2016), In situ hydrothermal syntheses, structures and photoluminescent properties of four novel metal-organic frameworks constructed by lanthanide (Ln=Ce(III), Pr(III), Eu(III)) and Cu(I) metals with

flexible dicarboxylate acids and piperazine-based ligands, Journal of Solid State Chemistry, 233, 415–421.

[105] Ay, B., Yildiz, E., Felts, A. C., Abboud, K. A., (2016), Hydrothermal synthesis, structure, heterogeneous catalytic activity and photoluminescent properties of a novel homoleptic Sm(III)-organic framework, Journal of Solid State Chemistry, 244, 61–68.

[106] Gunasekaran, S., Anita, B., Spectral investigation and normal coordinate analysis of piperazine, Indian Journal of Pure and Applied Physics, 46 (2008) 833–838.

[107] Ni, Y., Tao, J., Jin, J., Lu, C., Xu, Z., Xu, F., Kang, Z., (2014), An investigation of the effect of ligands on thermal stability of luminescent samarium complexes, Journal of Alloys and Compounds, 612, 349–354.

[108] Ay, B., Doğan, N., Yildiz, E., Kani, İ., (2015), A novel three dimensional samarium(III) coordination polymer with an unprecedented coordination mode of the 2,5-pyridinedicarboxylic acid ligand: Hydrothermal synthesis, crystal structure and luminescence property, Polyhedron, 88, 176–181.

[109] Li, M., Feng, R., Huang, Q. Z., Feng, Y. Q., Shi, H. Z., (2014), Synthesis, crystal structure and luminescent property of a novel lanthanide coordination polymer containing $(H_2O)_{20}$ clusters, Inorganic Chemistry Communications, 50, 8–12.

[110] Derakhshandeh, P. G., Soleimannejad, J., Janczak, J., (2017), Preparation of CeO_2 nanoparticles from a new cerium(III) supramolecular compound, Inorganica Chimica Acta, 467, 132–135.

[111] Ay, B., Yildiz, E., Kani, İ., (2018), Semiconducting lanthanide polymers of pyridine-2,6-dicarboxylate: Hydrothermal synthesis, structural characterization, electrical conductivity and luminescence properties, Polyhedron, 142, 1–8.

APPENDICES

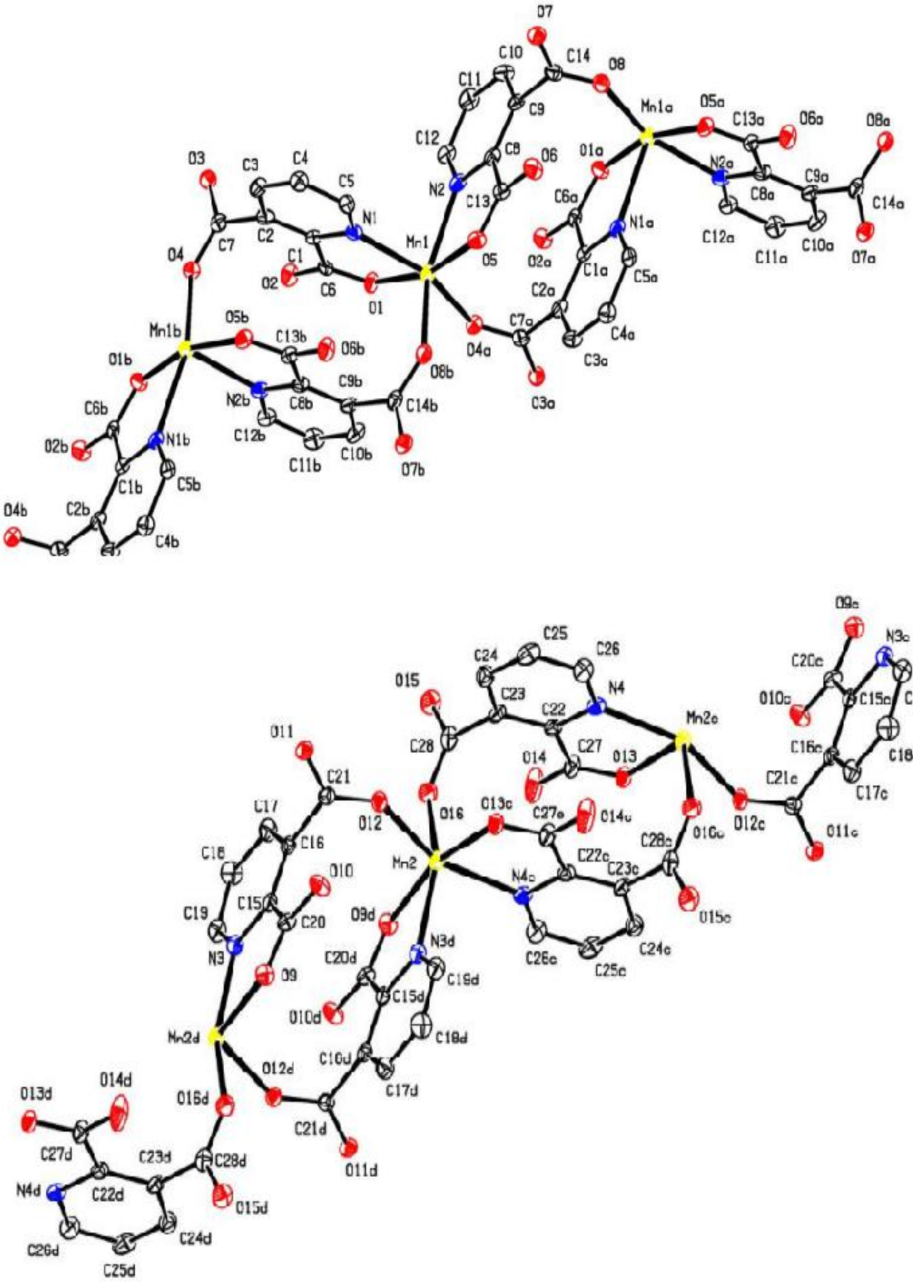

Figure A1. Polymeric chains of Mn^{2+} complex (**2**)

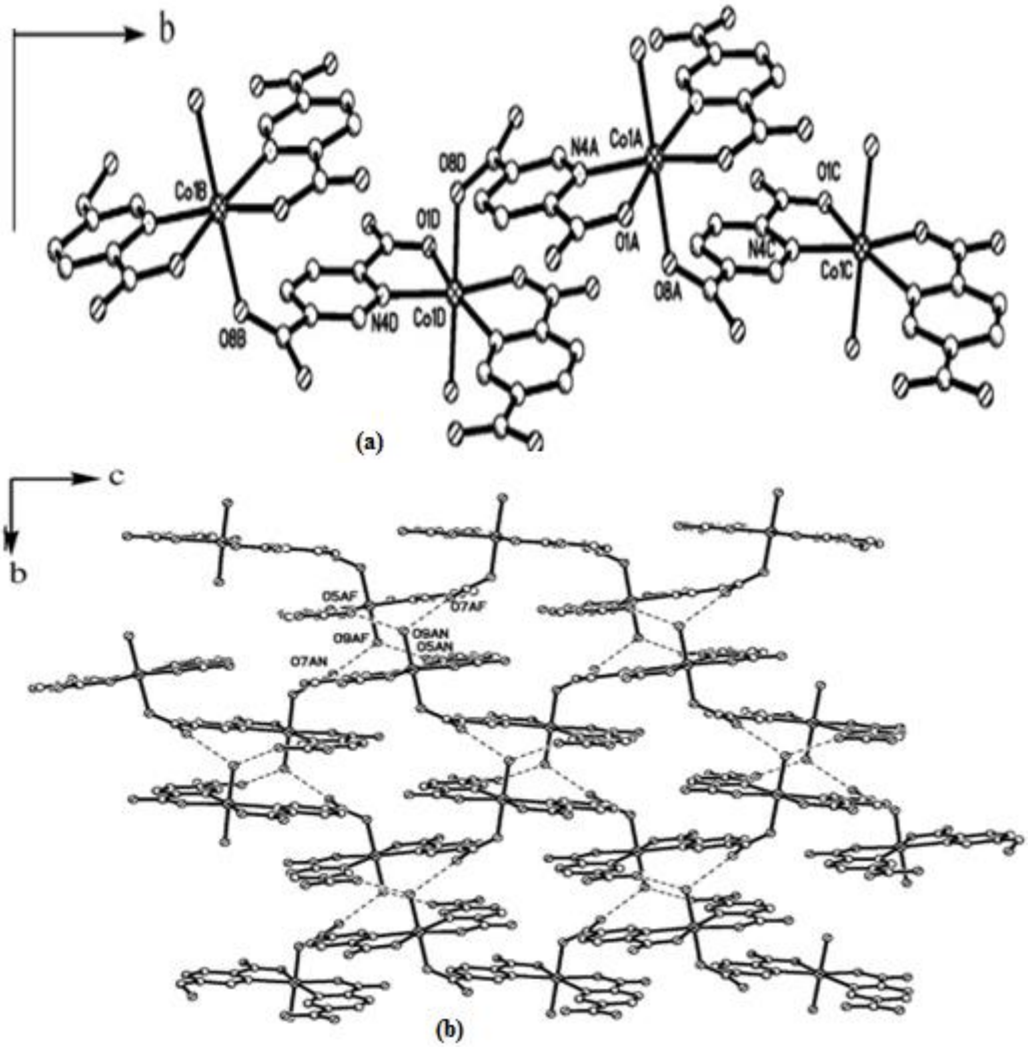

Figure A2. (a) The 1-D infinite chain of **5** along b-axis. (b) The 2-D H-bonded layer of **5** on bc plane

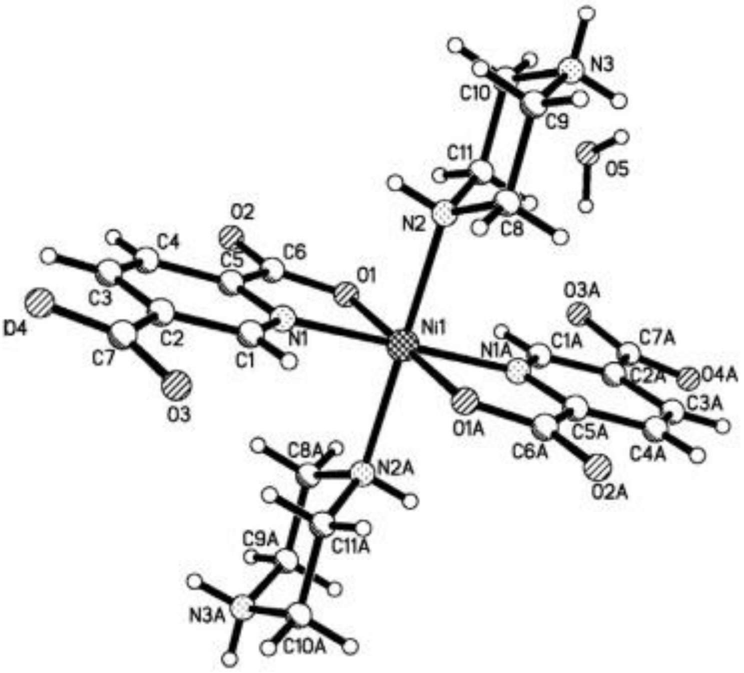

Figure A3. Molecular structure of $[Ni(Py\text{-}2,5\text{-}Dc)_2(HPpz)_2]\cdot H_2O$ (**6**)

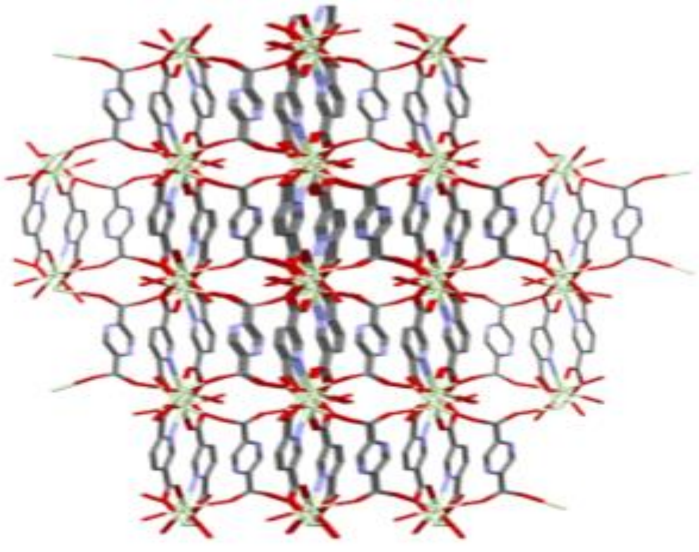

Figure A4. 3-D structure of compound **8**

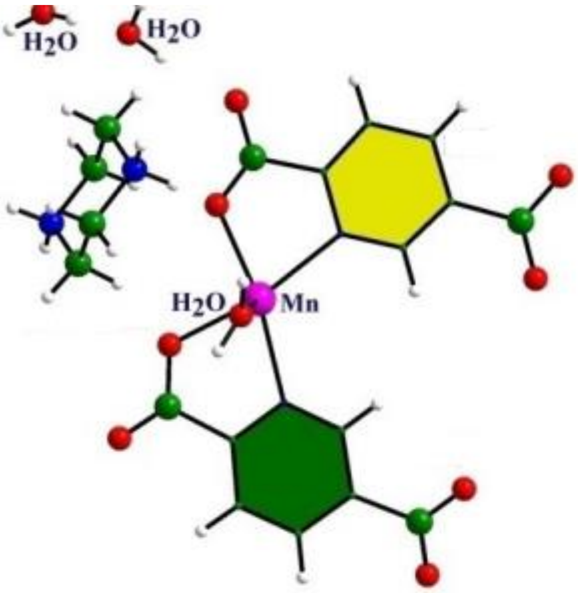

Figure A5. The asymmetric unit of {$(H_2Ppz)[Mn(Py\text{-}2,5\text{-}Dc)_2(H_2O)]\cdot 2H_2O$}(**9**)

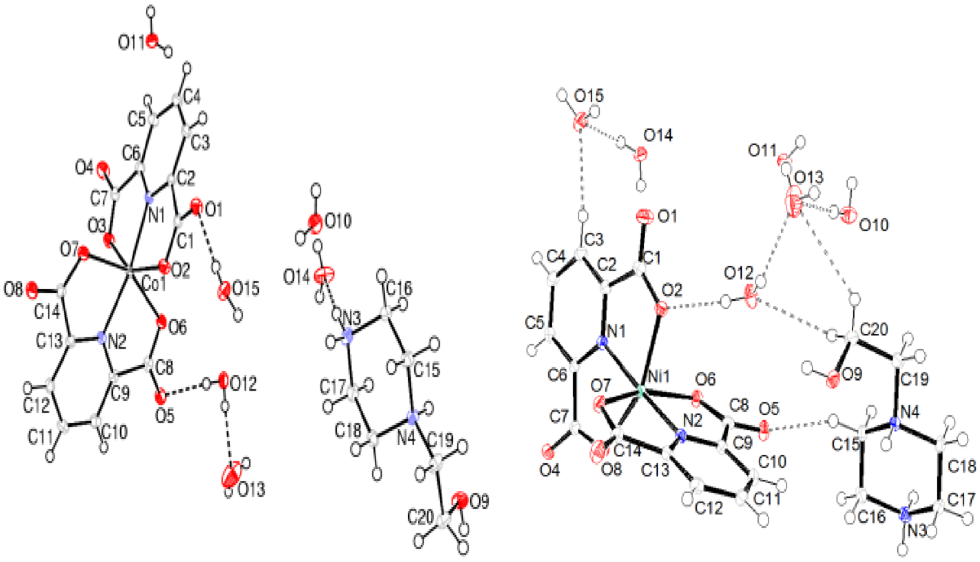

(a) (b)

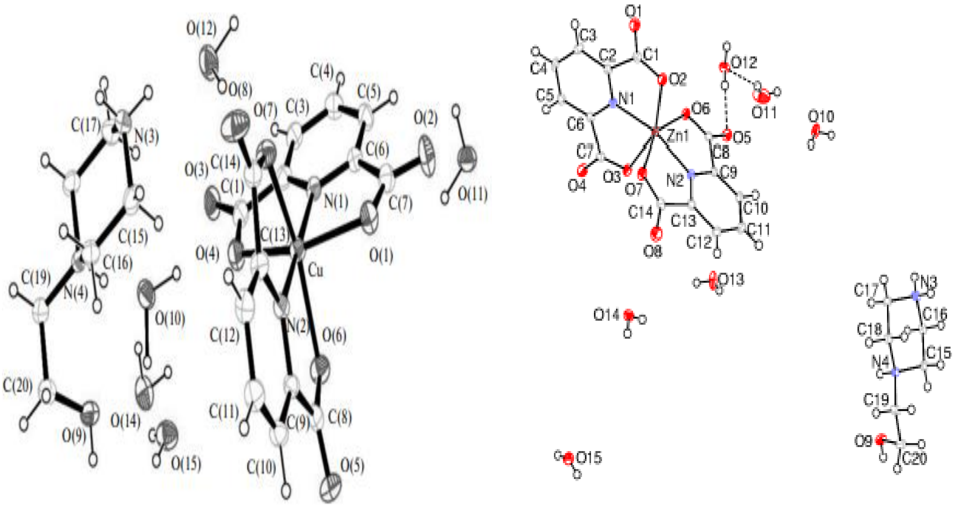

(c) (d)

Figure A6. Molecular structure of complexes (a) for **23**, (b) for **24**, (c) for **25** and (d) for **26**